NOAA Technical Memorandum NWS WR-137

LFM 24-HOUR PREDICTION OF EASTERN PACIFIC CYCLONES REFINED BY SATELLITE IMAGES

John R. Zimmerman and Charles P. Ruscha, Jr.
National Weather Service Forecast Office
Seattle, Washington

January 1979

UNITED STATES DEPARTMENT OF COMMERCE
Juanita M. Kreps, Secretary

NATIONAL OCEANIC AND ATMOSPHERIC ADMINISTRATION
Richard Frank, Administrator

NATIONAL WEATHER SERVICE
George P. Cressman, Director

This Technical Memorandum has been reviewed and is approved for publication by Scientific Services Division, Western Region.

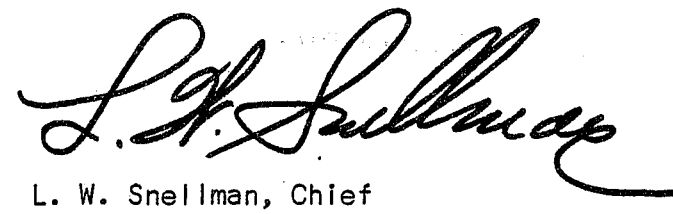

L. W. Snellman, Chief
Scientific Services Division
Western Region Headquarters
Salt Lake City, Utah

U.S. DEPARTMENT OF COMMERCE
National Oceanic and Atmospheric Administration
National Weather Service Western Region
P. O. Box 11188 Federal Building
Salt Lake City, Utah 84147

Date : May 1, 1979

Reply to Attn. of: WFW3

To : Recipients of NOAA Technical Memo NWS WR-137

L. W. Snellman

From : L. W. Snellman, Chief, Scientific Services Division

Subject: Errata Sheet to NOAA TM NWS WR-137: "LFM 24-hr Prediction of Eastern Pacific Cyclones Refined by Satellite Images"

Please make the following changes:

Page 20	Line 9, change 170W to 160W.
	Line 14, change 1200 GMT to 0600 GMT.
	Line 15, delete "at 47N 155W" and rewrite as: "the surface low center had deepened to 1004 mb at 50N 140W".
Page 21	Figure 37, change 1200 GMT to 0600 GMT.

cc: John Zimmerman and Charles Ruscha, Seattle WSFO

CONTENTS

FIGURES AND TABLES

FIGURES AND TABLES

Page

FIGURES AND TABLES

FIGURES AND TABLES

Page

LFM 24-HOUR PREDICTION OF EASTERN PACIFIC CYCLONES REFINED BY SATELLITE IMAGES

John R. Zimmerman and Charles P. Ruscha, Jr.
Weather Service Forecast Office
Seattle, Washington

ABSTRACT. In looking at Limited Fine Mesh (LFM) forecasts of surface cyclone central pressure, it was found that on eleven days between April and November 1977, observed surface cyclone central pressure was 10 mb or more lower than anticipated by the LFM model. These eleven cases were examined in detail.

A common property found on GOES satellite imagery at the time of undetected cyclone deepening in these eleven cases was the formation of a distinct, sharp, cloud-free slot region on the back side of the leaf-shaped clouds of the baroclinic zone. This feature was generally clearly detectable on infrared images.

For the period of data and subsequently, it was seen that as frequently as two or three times a month the LFM failed to predict significant cyclone development in the eastern Pacific. Satellite images provided the experienced meteorologist with evidence the cyclones would deepen when this development was not predicted by the LFM.

I. INTRODUCTION

Analysis and prognosis of surface weather charts at most National Weather Service (NWS) field stations have been automated. However, Seattle Ocean Services Unit (SOSU) routinely hand-plots and analyzes an in-house surface chart at 1800 GMT for specialized ocean forecasting applications. SOSU is a developmental group attempting to provide improved weather and oceanographic products for those who go to sea, whether it be for commerce, fishing, or pleasure. SOSU has found it advantageous to hand-analyze weather maps for the Pacific Ocean areas so that all reported ship and satellite interpretive data can be used. Much data, if late, may not be included in the automated analysis. The SOSU analysis allows special emphasis to be given to data of concern to mariners such as wind, sea and swell, and sea-surface temperature.

In the procedure developed to provide specialized marine forecasts for National Oceanic and Atmospheric Administration (NOAA) ships, the surface position of major storms in the Gulf of Alaska are drawn on a plastic overlay in black in order to obtain a history of their trajectories. In addition, the position of the jet stream aloft as given on the 300-mb chart is also drawn on the overlay in green, which helps to indicate possible regions of storm development and the storm's future trajectory. Finally, forecast LFM cyclone surface positions and intensity for the next two days for 1200 GMT are entered in yellow. After consulting all numerical guidance and checking history of the storm, the forecaster then makes his own subjective estimate of storm central pressure and position for the next two days valid at 1800 GMT each day.

Since operational weather guidance for the United States has become increasingly geared to output of the LFM model, the LFM was selected for cyclone forecasts rather than forecasts from the Primitive Equation coarse mesh (PE) model. It was recognized, however, that the western boundary of the LFM north of 35N extends from 160W at 35N to 150E north of 45N. Thus, weather systems in the extreme western Gulf of Alaska, will be near the LFM boundary and subject to computer boundary errors. Further investigation should compare LFM and PE forecasts in the extreme western Gulf of Alaska in order to determine the influence of boundary conditions on LFM predictions.

Forecast and observed positions and central pressure of surface low centers were kept in a log. This made it easy to compare the two forecasts and verify them against observed data. Furthermore, this information was useful for reference when predictions by either the forecaster or LFM were in gross error.

II. ACCURACY OF 24-HOUR FORECASTS OF CYCLONE CENTRAL PRESSURE AND POSITION

The data to be presented were taken from the period April 19 to November 21, 1977. Not all days were included, and operational and mainly eastern Pacific cyclones north of 35N latitude were verified. In the mean, forecast errors were slightly smaller than LFM errors for cyclone central pressure (about 0.5 mb better), but about the same for predicted 24-hour position of the surface cyclone (see Table 1). Of significance was how large the average forecast errors were for both cyclone central pressure and storm location, i.e., about 5 mb and 300 nm, respectively. These average errors for a 24-hour prediction are large and would be greater for a longer forecast period. In fact, there were many cases when storms in the eastern Pacific deepened 10 mb or more than the LFM had predicted (Figure 1).

	Human	LFM
Central pressure (mb)	4.9	5.4
Position (degrees of latitude)	3.7	3.8

Table 1. Mean absolute prediction errors of Human and LFM 24-hour forecasts of cyclone central pressure and position for the period April 9 to November 21, 1977.

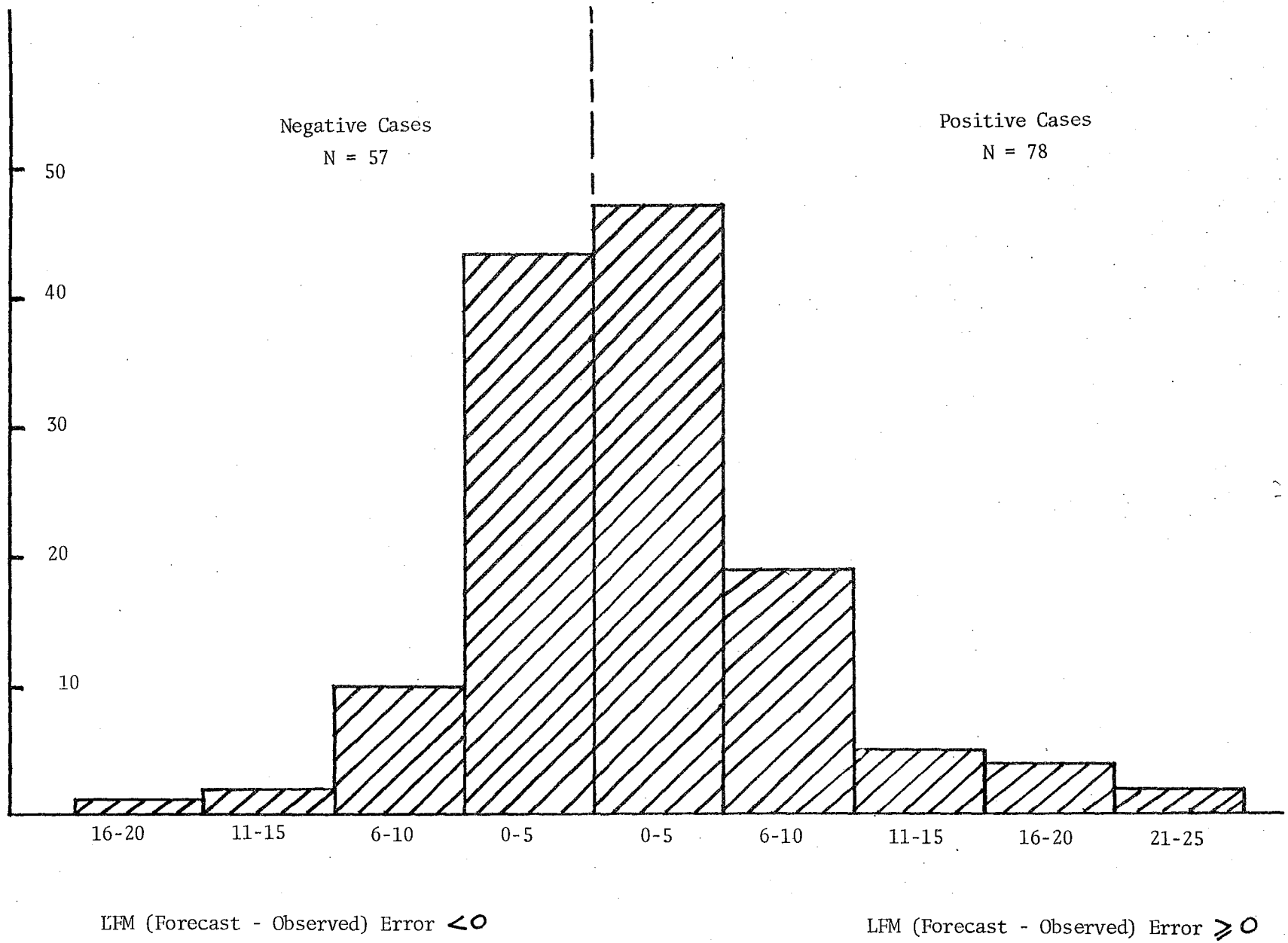

FIGURE 1. HISTOGRAM OF 24-HR LFM (FORECAST - OBSERVED) CYCLONE CENTRAL PRESSURE ERRORS FOR APRIL 19 TO NOVEMBER 21, 1977.

The sample showed (Table 2) that 24-hr LFM forecasts of cyclone central pressure minus observed cyclone central pressure was 10 mb or greater about twice per month. During this period there were 11 cases when cyclones deepened 10 to 24 mb more than predicted. Certainly, such failures to detect cyclone intensification can have serious consequences in terms of potential loss of life or damage to ships or cargo or both.

Date	P (12 GMT)	$\frac{\Delta P}{\Delta T}$ (24 hrs)	LFM Position Error ΔS (Degrees Latitude)	Forecast - Observed Pressure Error	
				LFM (12 GMT)	Human (18 GMT)
(1977)					
4/19	986	-14	7.2	10	12
5/4	964	-20	3.2	16	0
5/18	982	-18	3.2	12	5
6/3	992	-10	1.6	12	8
7/21	996	-24	2.5	13	8
9/1	1005	-11	7.5	14	2
9/26	980	-10	3.0	20	17
10/6	994	-10	2.1	12	16
10/14	958	-26	1.3	17	14
10/24	944	-36	0	24	23
11/18	968	-12	5.0	18	21

Table 2. Eleven cases when the 24-hr LFM (forecast - observed) cyclone central pressure error was 10 mb or more. All pressures and pressure changes are in millibars.

III. SYNOPTIC CHARTS ASSOCIATED WITH LARGE CYCLONE CENTRAL PRESSURE ERROR

The 500-mb patterns appear to be roughly similar regarding contour configuration and position of surface low-pressure centers relative to the 500-mb trough for the 11 cases when the LFM significantly underforecast cyclone central pressure. Surface low centers generally originated on the south side of the 500-mb trough, near the trough axis and traveled northeastward, north of the jet. As would be expected, cyclones of greater intensity developed under stronger 500-mb height gradients. With storm deepening there was always considerable cold-air advection in the 500-mb trough. (Refer to Figures 5, 8, 16, 22, 28, 35, 41, 47, 52, 57, 62.)

Likewise, characteristics of the developing surface low-pressure centers were roughly similar. These surface cyclones deepened from 15 to 35 mb per day, with a rapid eastward to northward movement of 30 knots or more (refer

to Figures 6, 7, 9, 10, 17, 18, 23, 24, 29, 30, 36, 37, 42, 43, 48, 49, 53, 54, 58, 59, 63, 64). Rapidly moving cyclones which deepened about 1-mb per hour for a full day resulted in radically altered weather conditions.

In Figure 2, it is seen that there is poor correlation between observed 24-hr pressure change and LFM central pressure error. For cyclone position, however, it is roughly true that the LFM cyclone position errors were smaller with greater 24-hr pressure changes, Figure 3.

Thus, it appears, for rapidly deepening storms, the LFM will predict cyclone central position with an acceptable degree of accuracy. Predicted cyclone central pressure, however, may be 20 mb or more too high. For weaker, smaller systems, the LFM poorly predicted both central pressure and location.

The initial analysis, either at surface level or aloft, is suspected as a probable cause of these misses. Rather than speculate about shortcomings of the LFM, however, it will be of greater value to look for techniques by which cyclone intensification can be anticipated by the forecaster when not handled well by the computer models.

IV. USING SATELLITE IMAGES FOR SHORT-PERIOD PREDICTION OF CYCLONE DEEPENING

In the short term (12-24 hours), satellite imagery has proven useful in determining the onset of cyclone development early enough to modify the LFM analysis when necessary. It goes without saying, that while attempting to modify the LFM forecast with satellite data, the LFM forecast should not be ignored. Even though not entirely accurate in intensity or timing of cyclone development, the LFM surface forecast does show the general trend of events.

Several recent satellite papers deal with satellite identification of cyclogenesis (Weldon 1977). For the 11 cases mentioned in Table 2, visible and infrared (IR) satellite images of the eastern Pacific and IR movie loops were viewed to examine the sequence of cloud patterns during cyclone development.

Perhaps the most obvious clues common to all these cases of cyclone deepening was the formation of a distinct concave cloud edge on the poleward side (colder side of jet stream) of the cirrus clouds associated with the baroclinic zone, and the subsequent formation of a "clear slot" on IR pictures. The clear slot or surge zone as described by Weldon (1976) is that region located just to the rear of the baroclinic cloud pattern or to rear of the concave portion of the comma cloud. This is also the region of the baroclinic zone where translation of cloud elements is the greatest. In our study cyclogenesis or cyclone deepening took place whenever a slot was detected by the analyst. A distinct increase in sharpness occurred along the back edge of the cloud pattern which extended along the concave

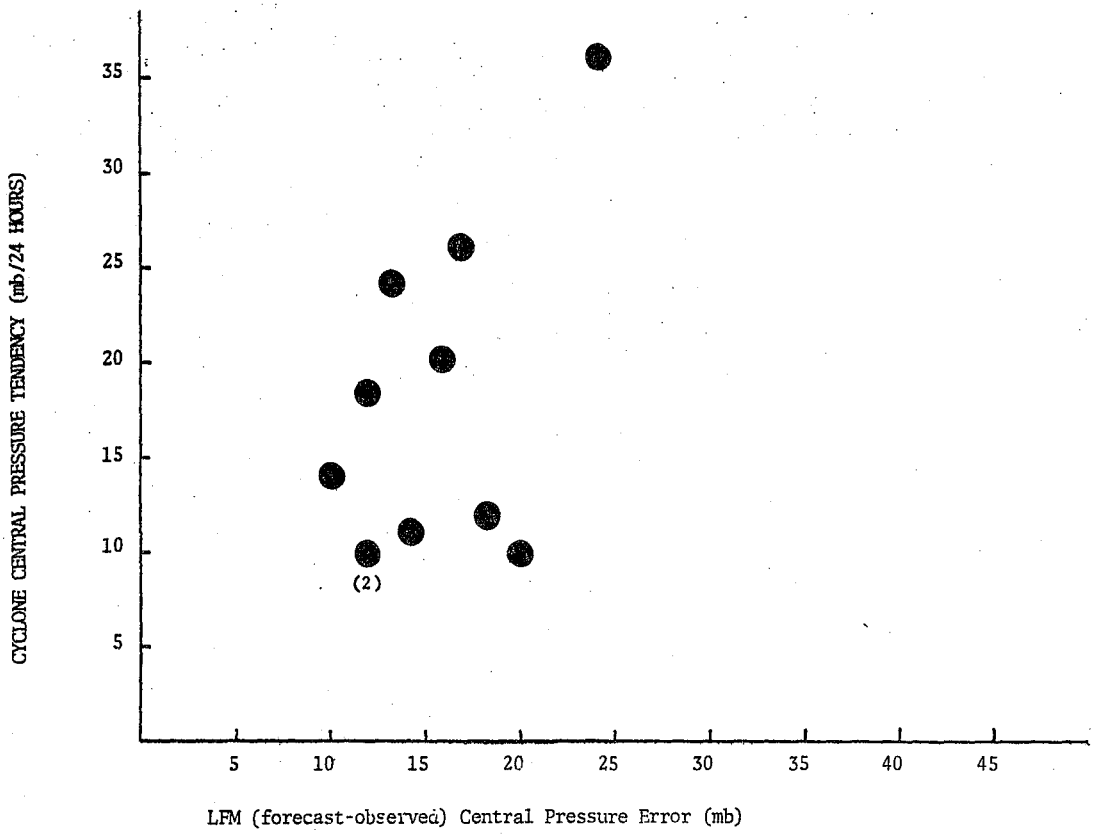

Figure 2

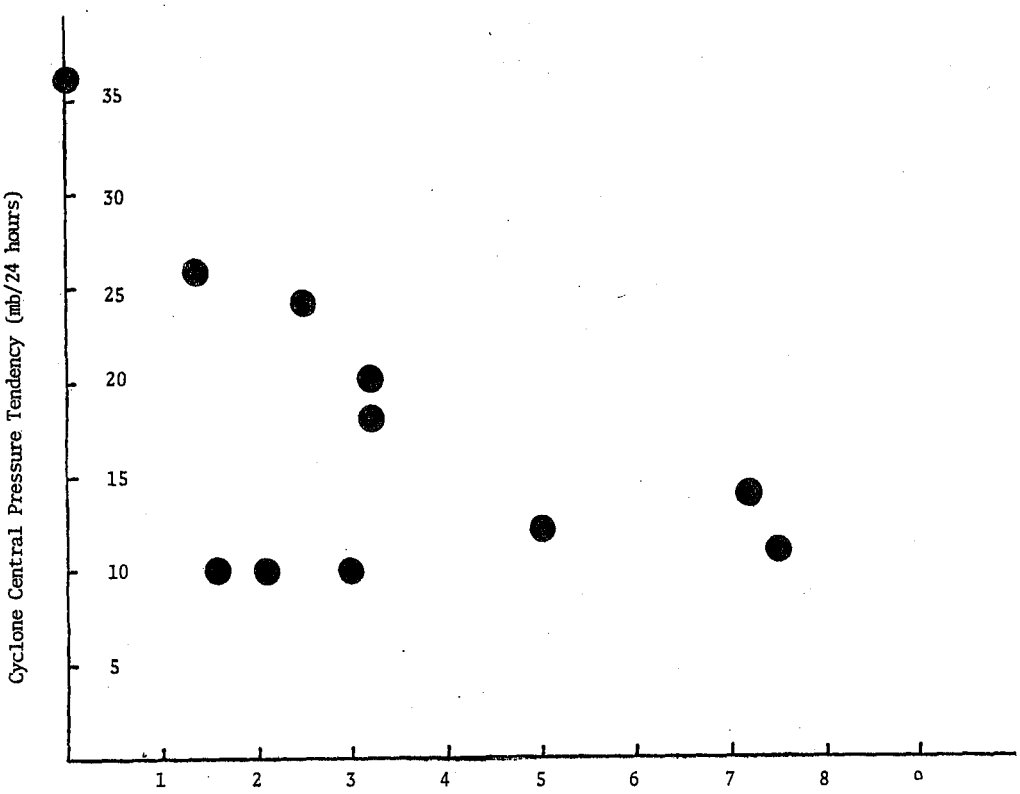

Figure 3

portion of the comma cloud toward its tail. Figure 4 shows a simplified model of a comma cloud pattern which indicates the location of the slot along the back edge of the comma cloud. The slot, more detectable on IR pictures than visible images, evolved into many different sizes and shapes. It was easily identified and provided visual evidence of the various stages of cyclone development.

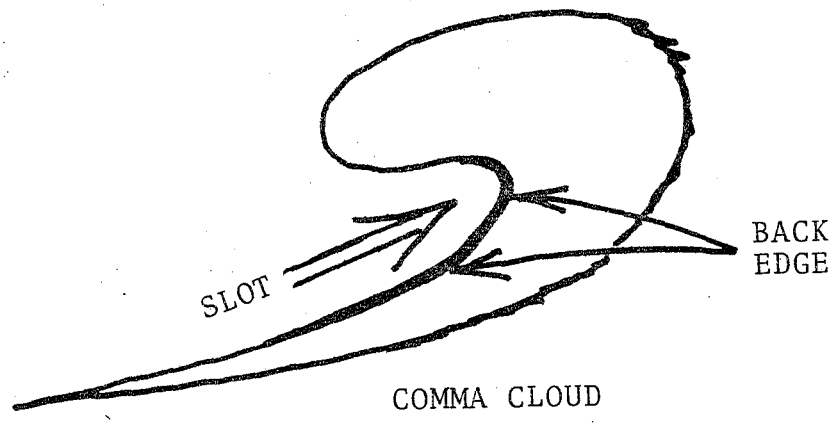

Figure 4.

The relative intensity of the cyclone was indicated by two observable features: 1) Sharpness of the back of the comma cloud edge and 2) the degree of whiteness (colder cloud-top temperature) of the cirrus clouds near the edge. With larger, deeper systems, a large cluster of open cellular clouds follows the comma cloud.

Most patterns were complex containing interacting systems. There were fewer instances when the satellite picture showed a relatively simple or "ideal" sequence of events as is commonly modeled. The term "ideal" will be used for isolated, large storms. Instances of this type occurred October 14, Figure 5 - 7, and again October 24, Figures 8 - 10.

V. EXAMPLE OF "IDEAL" CYCLOGENESIS

A pronounced baroclinic zone stretched across the Pacific from 160E to 140W longitude between 35N to 50N latitude on 500-mb charts from October 21 - 25. Still satellite images at 2345 GMT each day for this period are shown in Figures 11 - 14. The first hint of a new storm developing was the "leaf" shaped cloud mass off the left side of the picture near 40N 180W on October 21. This system moved eastward about 25 knots along 40N latitude.

By October 22 the cloud structure had sharpened on the poleward side of the leaf pattern and a dry slot had formed. On October 23 the storm continued to deepen. The cold front, now very distinct, contained a narrow clear zone on its poleward side. Numerous cumulus cells were

visible in the cold air advected southeastward behind the cold front. The cold front appeared as a smooth, curved line extending from about 47N 141W to 29N 178W, a distance of about 2000 miles. No frontal waves developed as it sped eastward across the Pacific about 15 degrees of longitude per day.

Finally, on October 24 the storm was fully mature and had a central pressure of 944 mb (Figure 10). A new cyclone had begun to form over the Aleutian Chain and was cutting off the cold air behind the storm in the eastern Pacific. Decay of the storm occurred as its cold air supply was blocked by warm-air advection ahead of the young cyclone which formed upstream.

Film loops covering this period confirm that this "ideal" case of cyclogenesis was quite similar to the model of cyclogenesis proposed by Weldon (1977). The baroclinic leaf-shaped clouds of bright, high-cirrus clouds sharpened on the poleward side prior to the formation of a surge zone. As the surge zone or slot developed, the rear portion of the cloud leaf dissipated and a long, narrow cold front became visible as indicated by a thin line of gray clouds. The surface frontal zone remained narrow, stretched by the deformation of the low-level winds, with cloud elements moving both northeastward toward the slot and southwestward behind the cold front.

An extremely large area of open cellular cumulus clouds which covered the entire eastern Pacific area existed in the cold air to the north of the frontal cloud band. To the southeast, considerable amounts of low clouds streamed northeastward in the warm subtropical air ahead and along the cold front.

A section of the 1800 GMT surface chart of October 24, with ship reports plotted in the usual station model format is shown in Figure 15. Many ships near the center of this storm experienced winds greater than 50 knots and monstrous seas 30 to 40 feet or higher. United States Geological Survey (USGS) ship R/V SP LEE receiving SOSU marine forecasts, radioed the following weather reports October 24.

Time (GMT)	Latitude/ Longitude	Wind (kt)	Pressure (mb)	Seas (ft)	Swells (ft)
06	43.9/137.6	270/70	980	57	49
12	43.5/137.6	250/60	992	46	52
15	43.5/137.7	260/55	997	26	44
18	43.4/138.1	230/48	1000	26	41
21	43.4/137.9	260/50	1000	26	41

These reports of seas and swells 40 - 50 ft high were so startling, that the forecaster, believing a coding error had occurred, requested and received confirmation that the reports were transmitted correctly. Swells from this storm were in excess of 20 ft (Table 3) along the Washington and Oregon coast. In this case of strong cyclogenesis, the position of the storm was accurately predicted by the LFM, but in 24 hrs its central pressure fell 24 mb lower than was forecast.

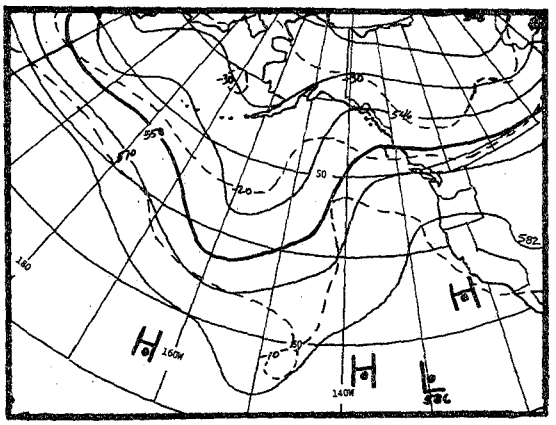

Figure 5. 500-mb Analysis, 10/14/77, 0000 GMT.

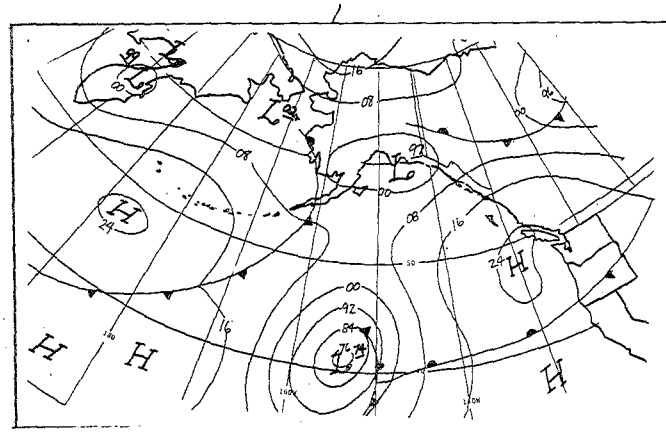

Figure 6. Surface Analysis, 10/13/77, 1200 GMT.

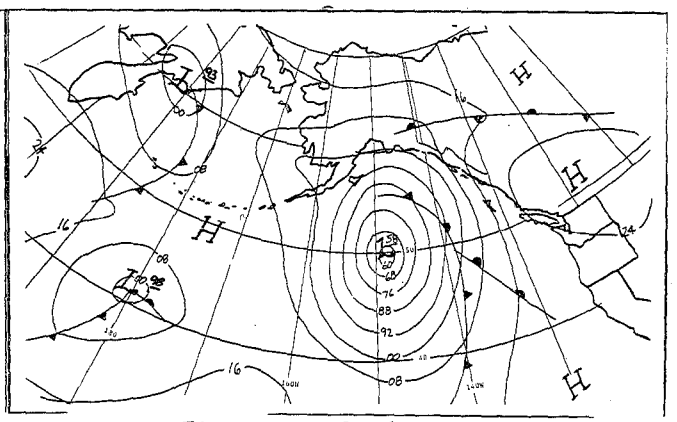

Figure 7. Surface Analysis, 10/14/77, 1200 GMT.

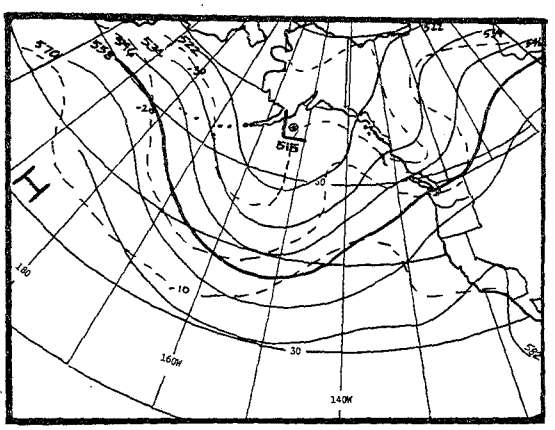

Figure 8. 500-mb Analysis, 10/24/77, 0000 GMT.

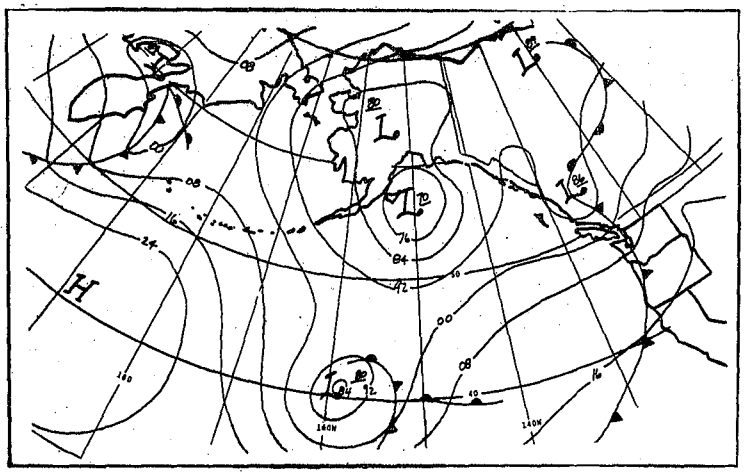

Figure 9. Surface Analysis, 10/23/77, 1200 GMT.

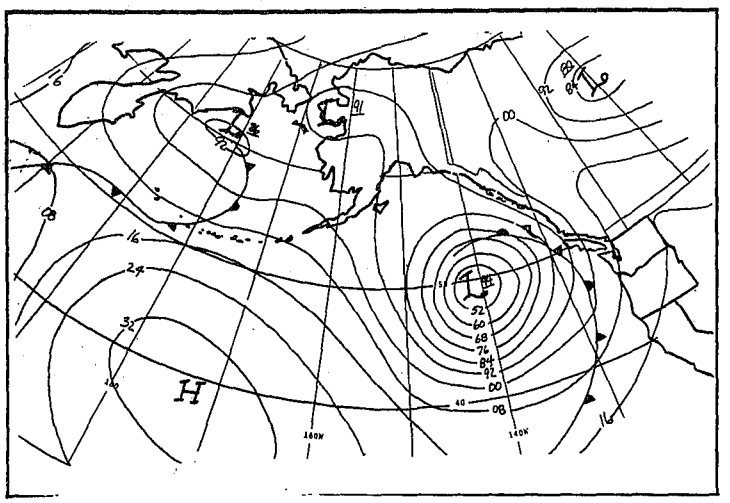

Figure 10. Surface Analysis, 10/24/77, 1200 GMT.

STATION	HIGHEST SWELL (ft)
Quillayute	22
Cape Disappointment	20
Yaquina Bay	19
Coos Bay	18
Chetco River	20

Table 3. Highest reported swell along the Washington-Oregon coast on October 25, 1977. Swells were measured by wave meter.

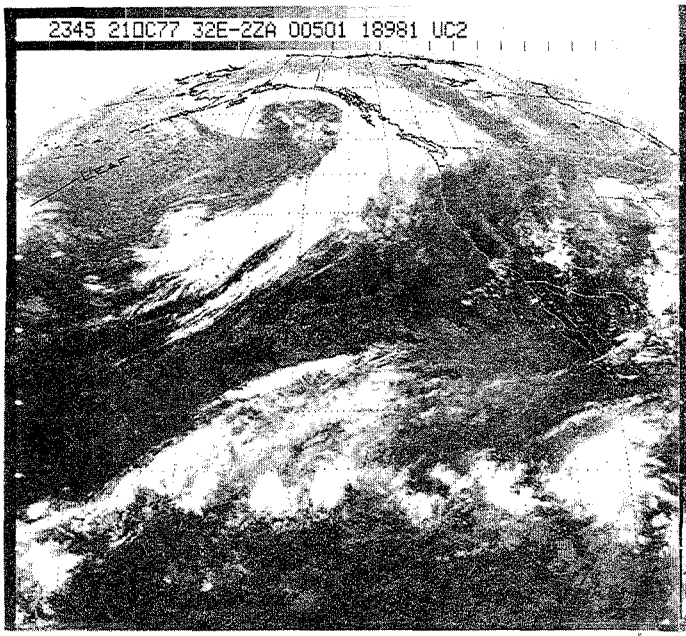

FIGURE 11. SATELLITE IMAGE OF CYCLONE DEVELOPMENT. OCTOBER 21, 1977, 2345 GMT.

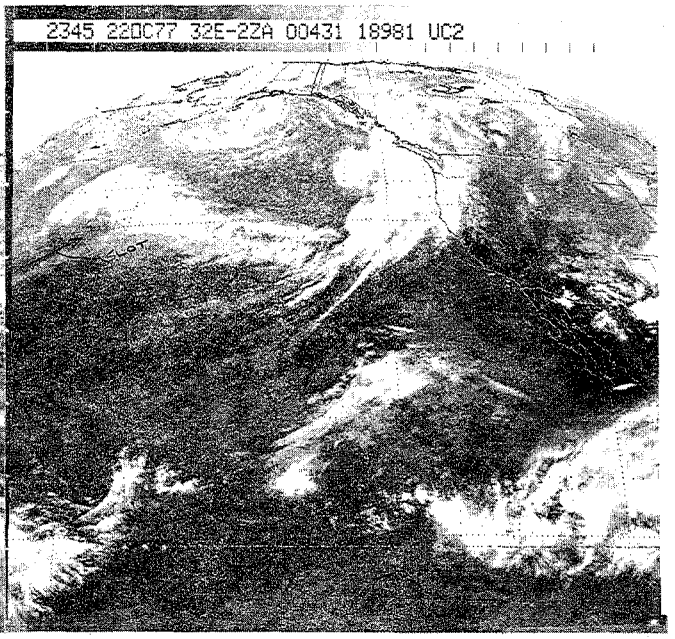

FIGURE 12. SATELLITE IMAGE OF CYCLONE DEVELOPMENT, OCTOBER 22, 1977, 2345 GMT.

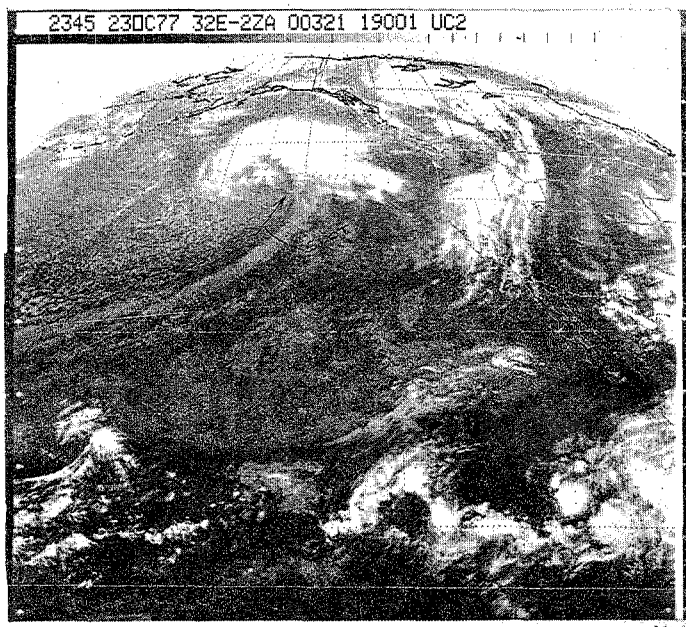

FIGURE 13. SATELLITE IMAGE OF CYCLONE DEVELOPMENT, OCTOBER 23, 1977, 2345 GMT.

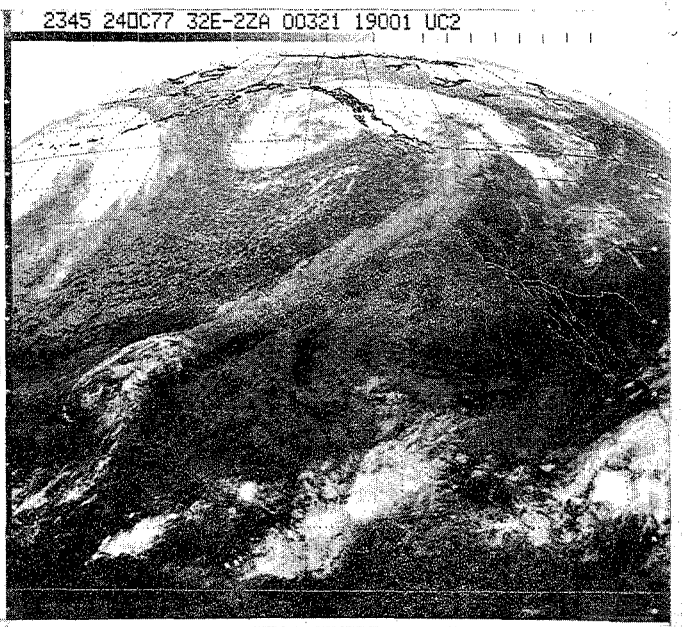

FIGURE 14. SATELLITE IMAGE OF CYCLONE DEVELOPMENT, OCTOBER 24, 1977, 2345 GMT.

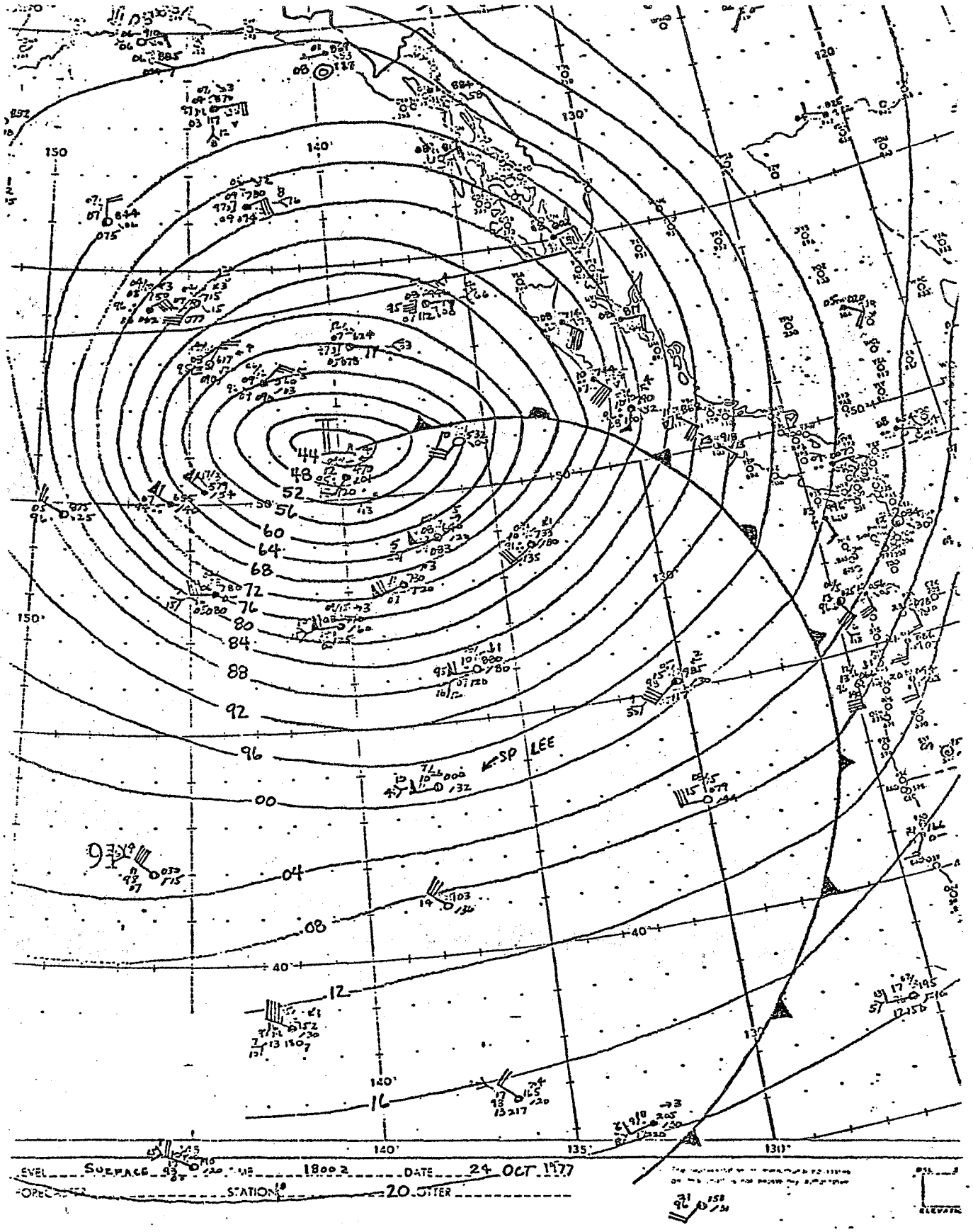

Figure 15. Surface Analysis, 10/24/77, 1800 GMT.

VI. EXAMPLES OF CYCLONE DEEPENING DIFFERENT FROM "IDEAL" CYCLOGENESIS

When cyclone deepening occurred, in most instances it behaved differently from the sequence of events described by "ideal" cyclogenesis. Usually, a mature storm was already present (or combination of old storm systems) and cyclogenesis, or cyclone deepening, took place in the southwest quadrant of a large low pressure trough aloft. It is this non-"ideal" behavior which the LFM predicts poorest. In many cases, rapid development took place in only 12 hours.

Case of May 17

A long baroclinic zone oriented north-south along 155W stretched from 40N to 50N on May 17 at 1545 GMT (Figure 19). An elongated north-south slot extended parallel to it on the north side. Near 45N 155W a strong speed max was apparent at point A. As this speed max reached the slot, a new slot formed near 51N at 2345 GMT (see satellite imagery, Figures 20 and 21, and 500-mb analysis, Figure 16).

At the surface a 998-mb low located near 44N 161W on May 17, at 1200 GMT, moved northward about 35 knots (Figure 17). In 24 hours its central pressure dropped 16 mb to 982 mb (Figure 18).

Deepening of the low center in this case could have been anticipated by the sharpening of the edge of cirrus clouds bordering the slot and its subsequent rotation. The direction of the low was indicated by the orientation of the slot.

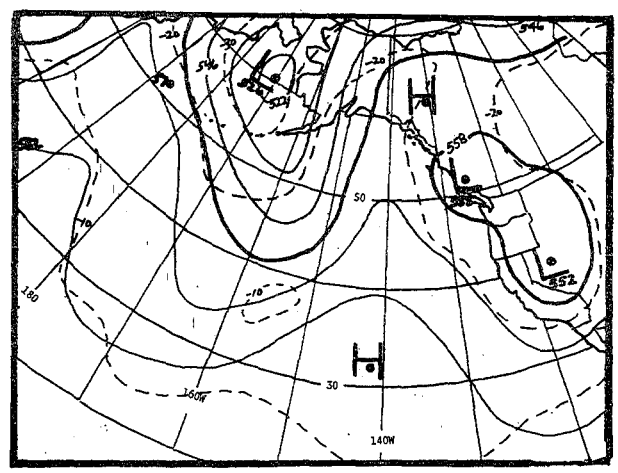

Figure 16. 500-mb Analysis, 5/18/77, 0000 GMT.

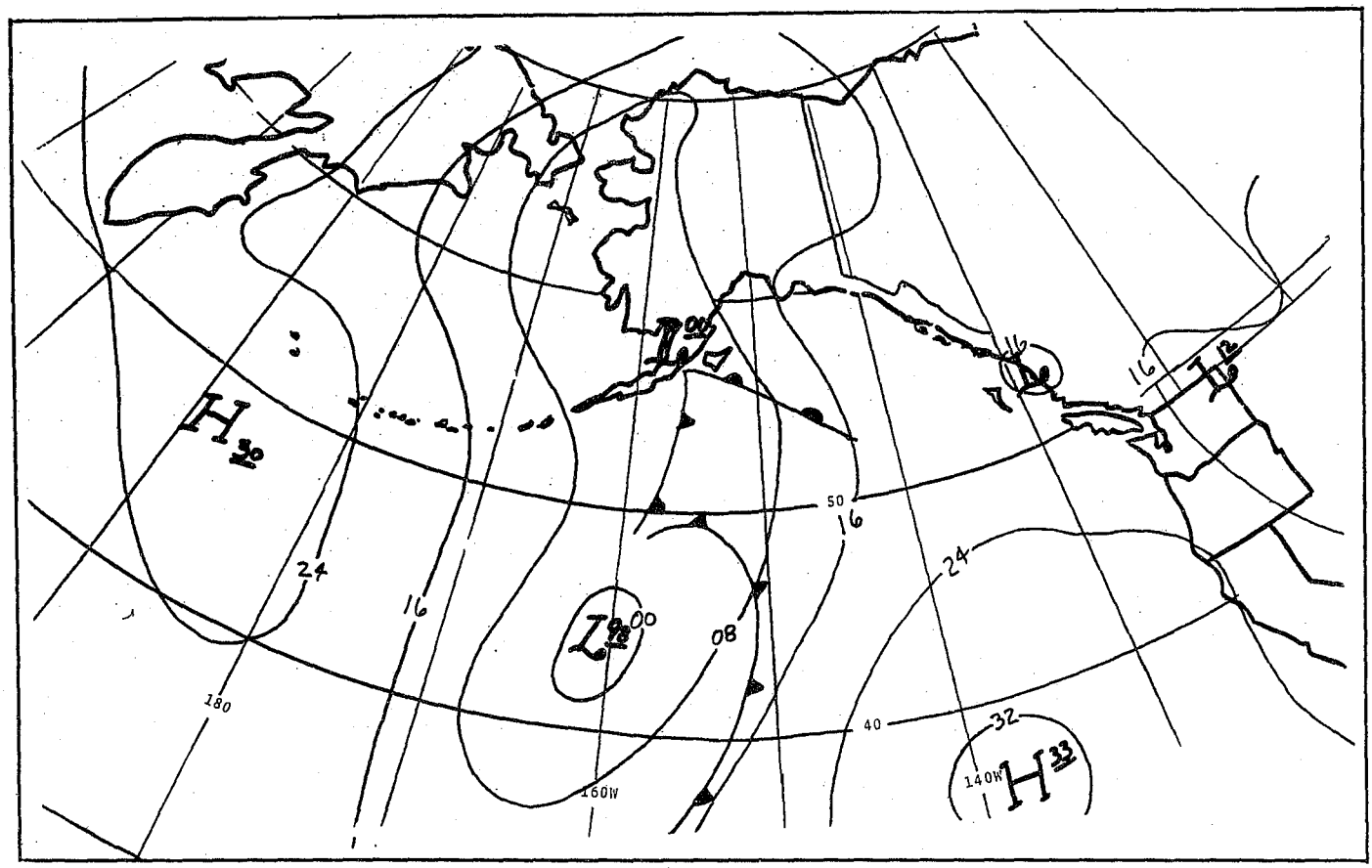

Figure 17. Surface Analysis, May 17, 1977, 1200 GMT.

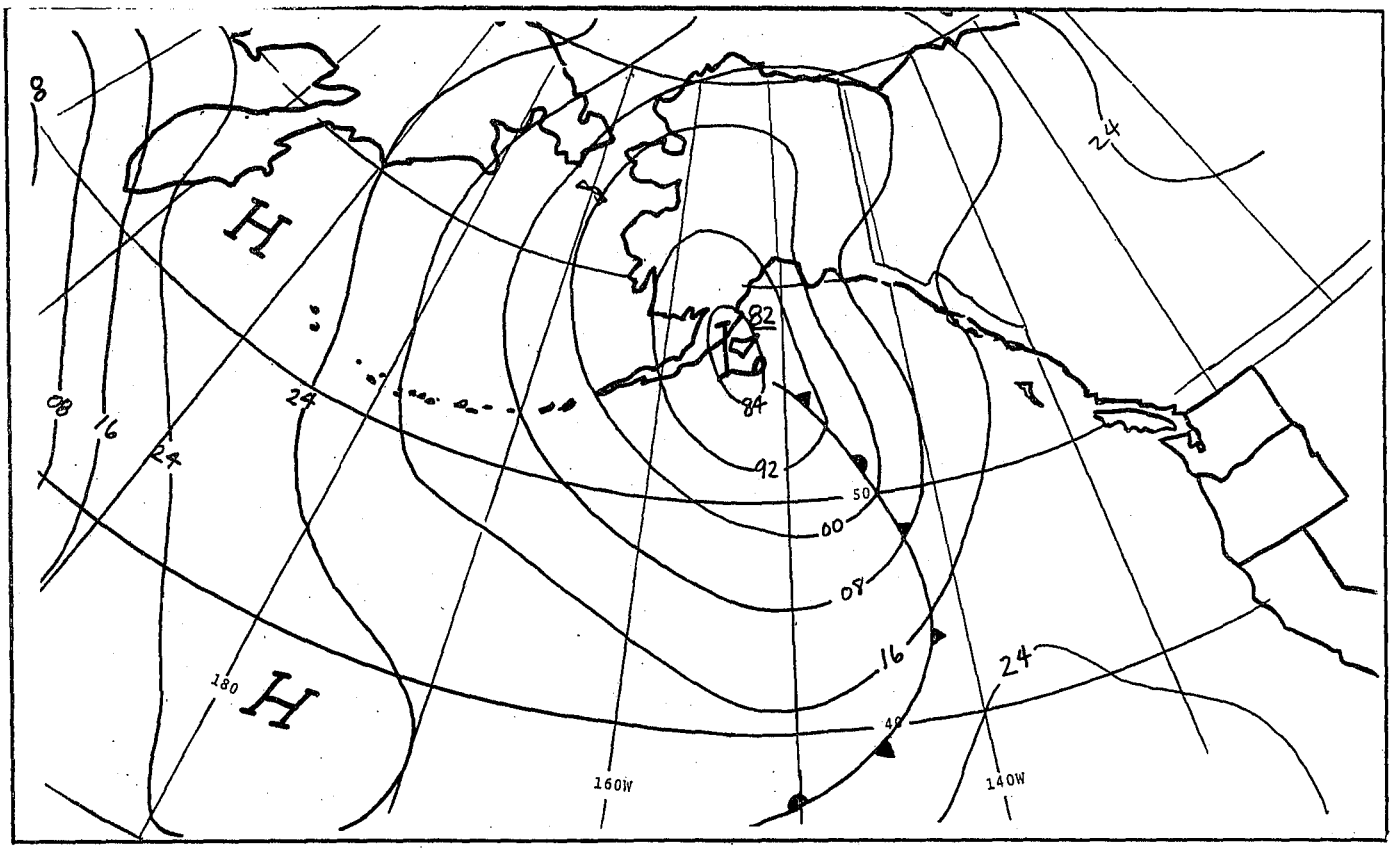

Figure 18. Surface Analysis, May 18, 1977, 1200 GMT.

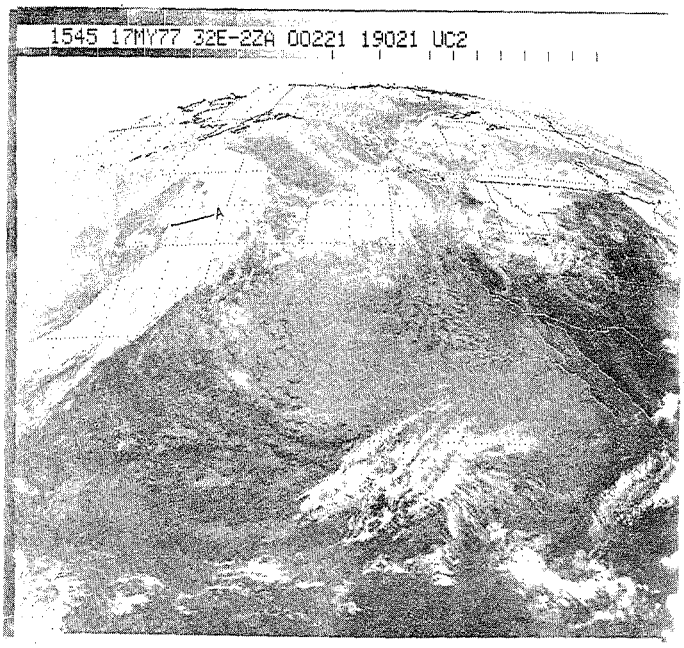

FIGURE 19. SATELLITE IMAGE OF CYCLONE DEVELOPMENT, MAY 17, 1977, 1545 GMT.

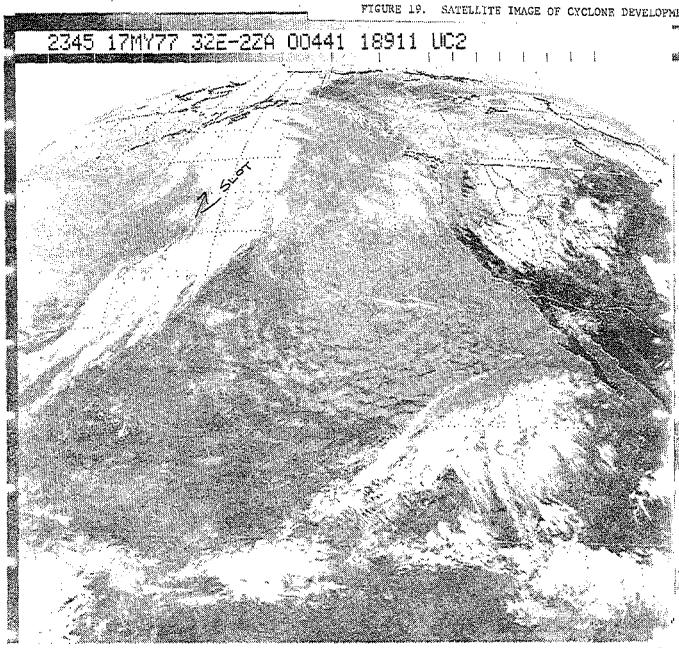

FIGURE 20. SATELLITE IMAGE OF CYCLONE DEVELOPMENT, MAY 17, 1977, 2345 GMT.

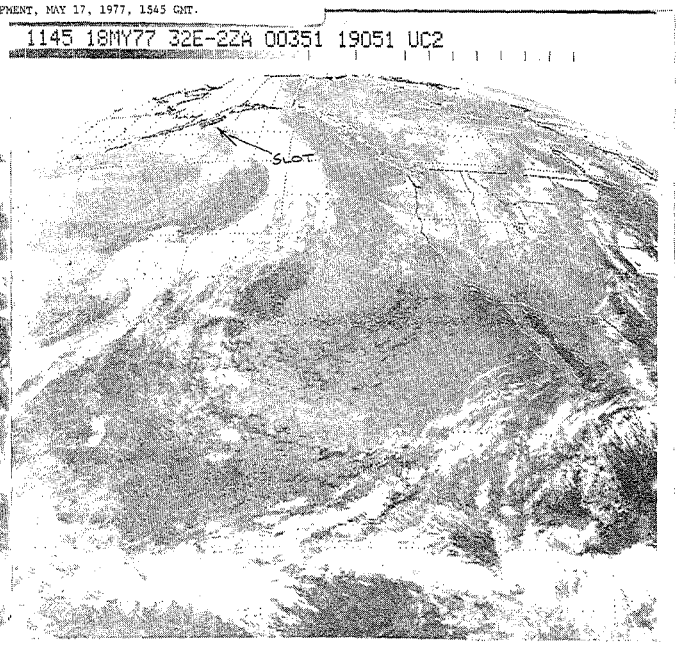

FIGURE 21. SATELLITE IMAGE OF CYCLONE DEVELOPMENT, MAY 18, 1977, 1145 GMT.

Case of June 2

A 1002-mb surface low was centered near 44N 159W on June 2, 1200 GMT, embedded in a broad zonal flow aloft (Figures 22 and 23). This system translated rapidly eastward. At 1145 GMT, June 2, a large leaf-shaped cloud mass was present near 40N 140W (point B, Figure 25). Farther southwest a cloud pattern normally associated with a wind maxima along the jet stream was evident along 40N (point A, Figure 25). Speed of the jet was estimated by satellite-derived winds to be at least 150 kt. By 1445 GMT (Figure 26) IR data showed the slot to be less distinct; however, it was well defined on visible imagery at 1815 GMT (Figure 27). The surface-pressure analysis for June 3, 0600 GMT (Figure 24) showed a low center at 992 mb at 44N 142W which was 10 mb lower than predicted.

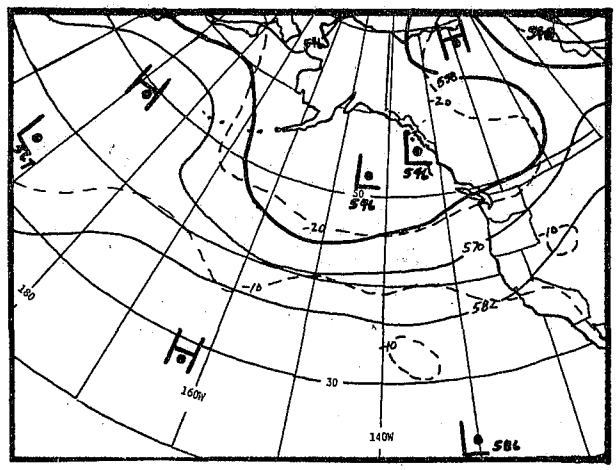

Figure 22. 500-mb Analysis, 6/3/77, 0000 GMT.

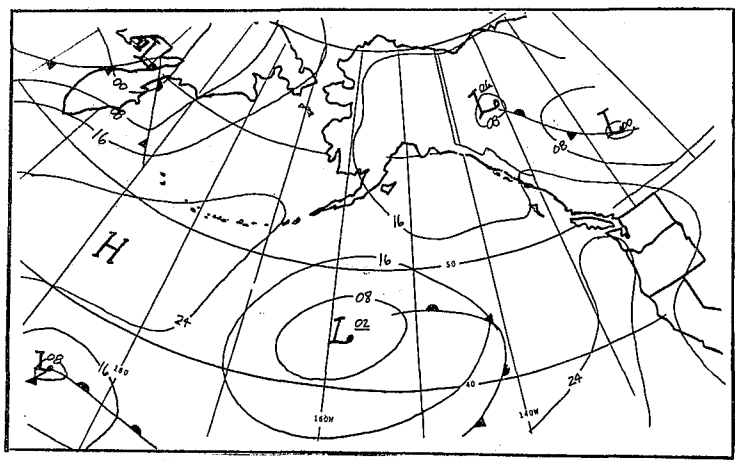

Figure 23. Surface Analysis, 6/2/77, 1200 GMT.

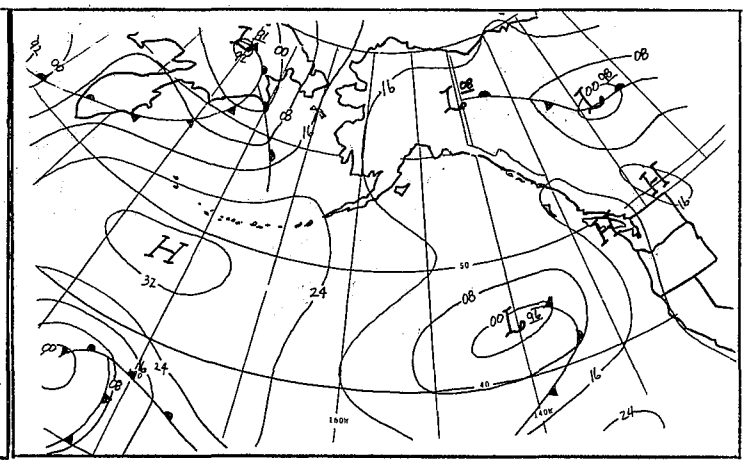

Figure 24. Surface Analysis, 6/3/77, 0600 GMT.

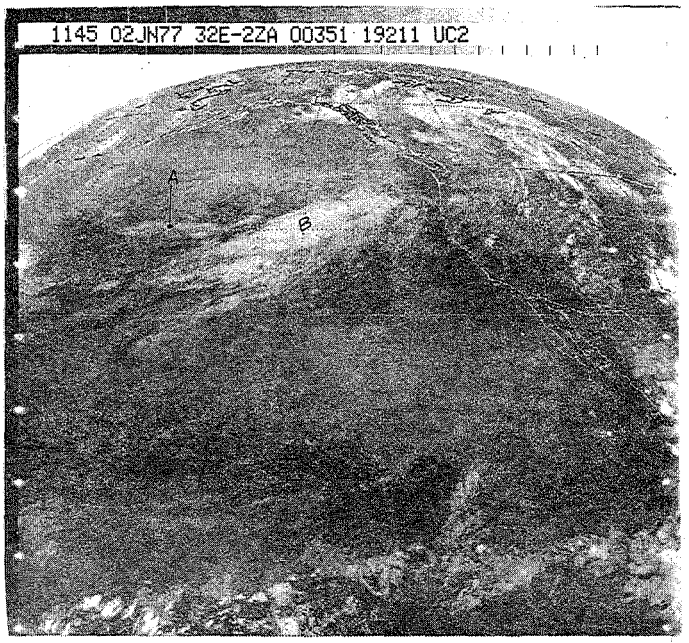

FIGURE 25. SATELLITE IMAGE OF CYCLONE DEVELOPMENT, JUNE 2, 1977, 1145 GMT.

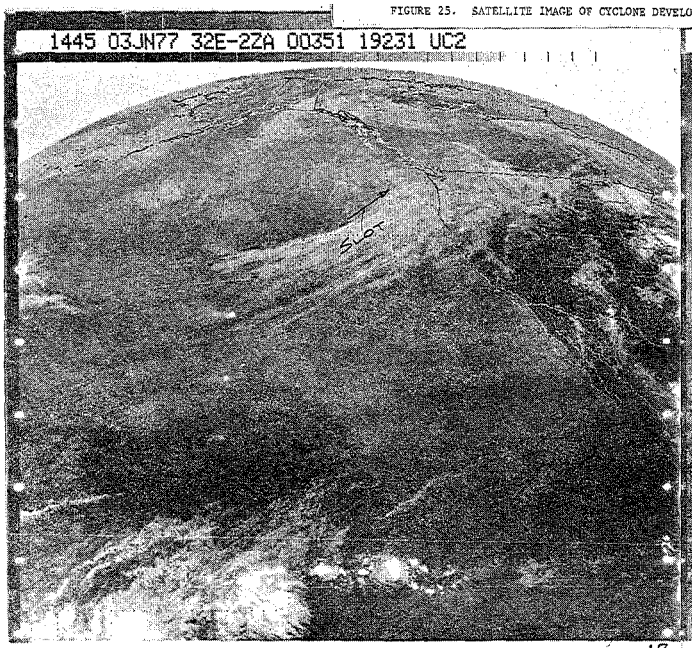

FIGURE 26. SATELLITE IMAGE OF CYCLONE DEVELOPMENT, JUNE 3, 1977, 1445 GMT.

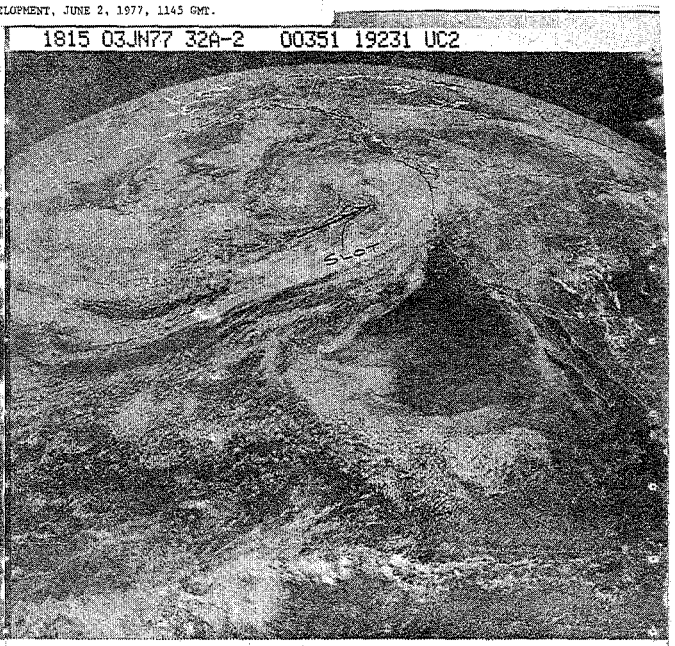

FIGURE 27. SATELLITE IMAGE OF CYCLONE DEVELOPMENT, JUNE 3, 1977, 1815 GMT.

Case of July 20

A baroclinic cloud leaf was visible at the top left edge of the satellite picture on July 20 at 1745 GMT (Figure 31). A weak wave, associated with the cloud feature, was analyzed at 50N 177W on the 1800 GMT surface chart, Figures 28 and 29. By 2345 GMT, a slot was evident near point A, Figure 32. In the next 12 hours the slot grew rapidly and by 1145 GMT on July 21 the concave back edge had moved eastward to 51N 165W (Figure 33). On this picture the back edge of the slot south of 50N was noticeably sharper and more distinct. On the surface chart at 1800 GMT the low-pressure center had deepened 24 mb in 24 hours to a central pressure of 994 mb (Figure 30). In the next 24 hours the slot continued moving eastward and its strength was maintained. This was a moderately intense system for mid-summer.

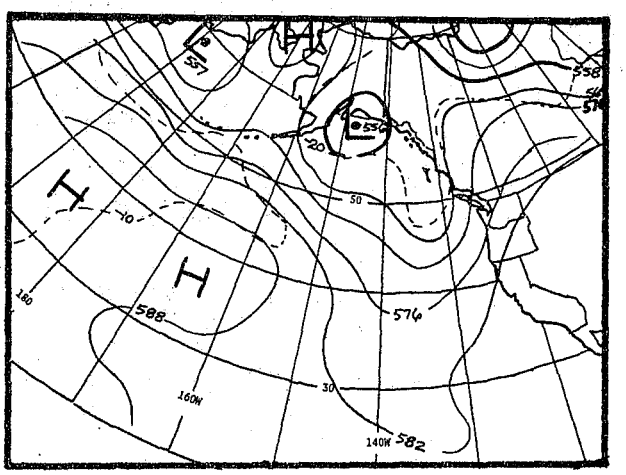

Figure 28. 500-mb Analysis, 7/20/77, 0000 GMT.

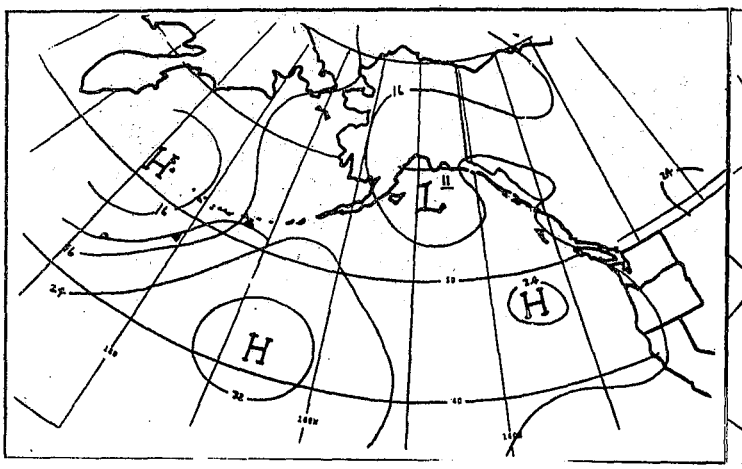

Figure 29. Surface Analysis, 7/20/77, 1800 GMT.

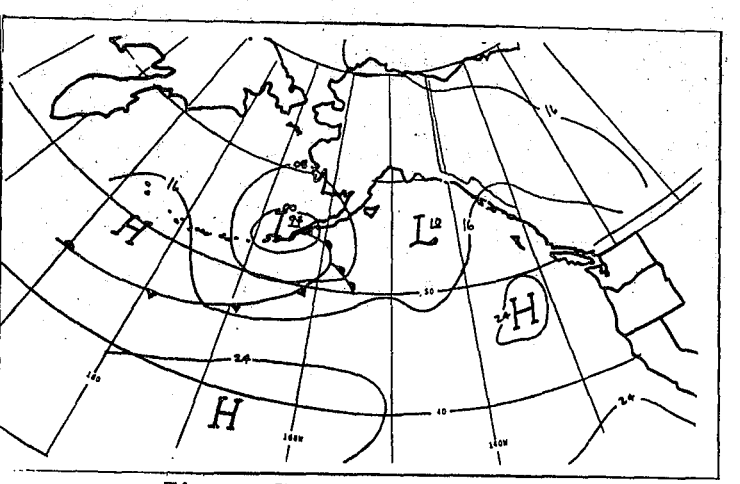

Figure 30. Surface Analysis, 7/21/77, 1800 GMT.

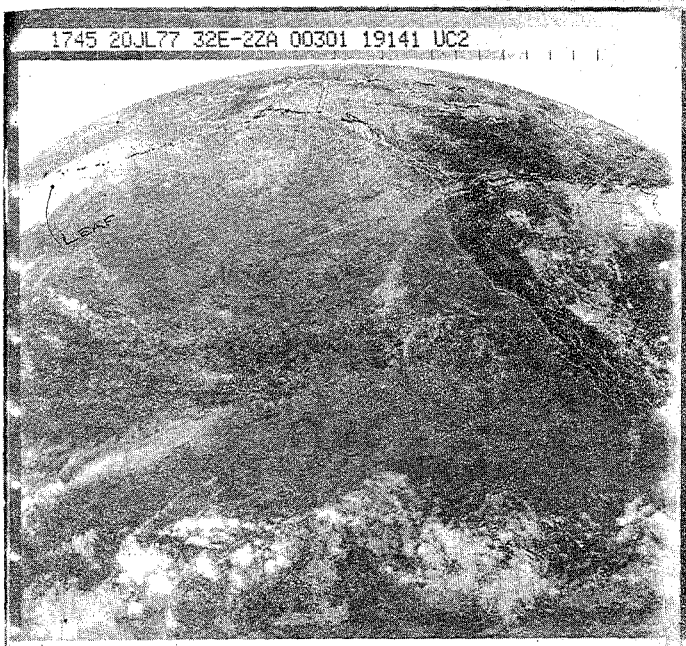

FIGURE 31. SATELLITE IMAGE OF CYCLONE DEVELOPMENT, JULY 20, 1977, 1745 GMT.

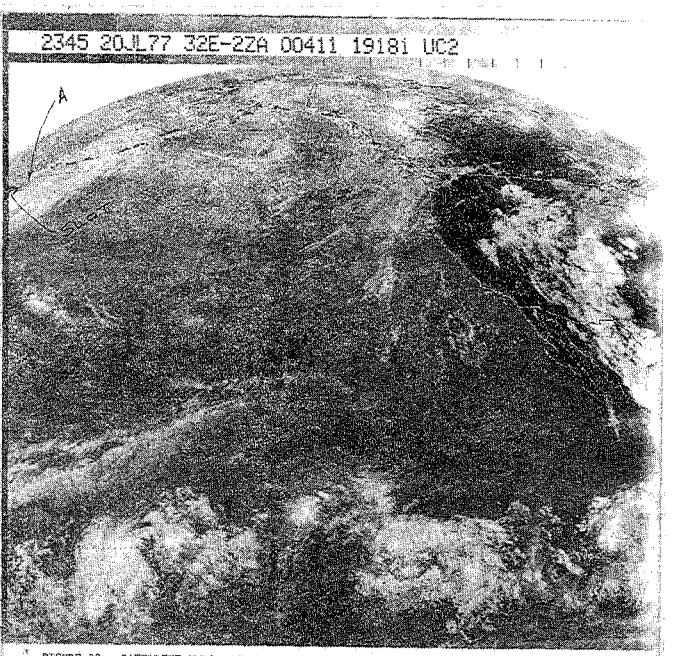

FIGURE 32. SATELLITE IMAGE OF CYCLONE DEVELOPMENT, JULY 20, 1977, 2345 GMT.

FIGURE 33. SATELLITE IMAGE OF CYCLONE DEVELOPMENT, JULY 21, 1977, 1145 GMT.

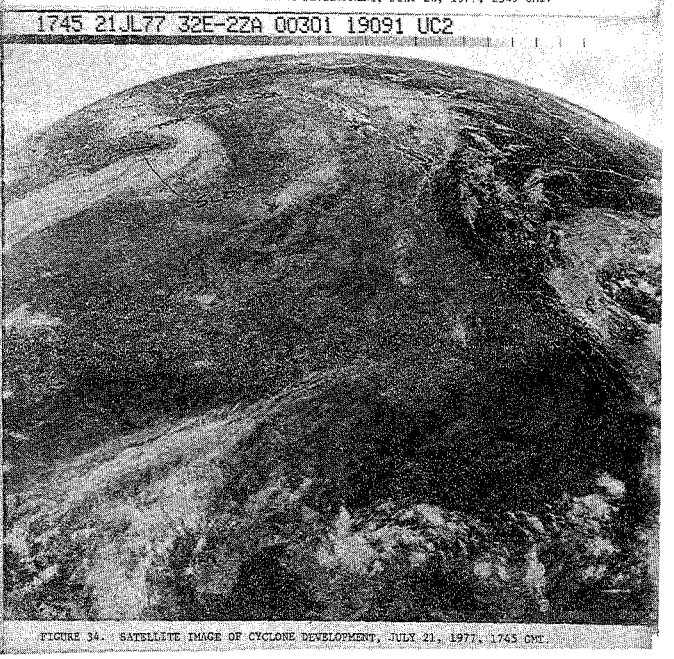

FIGURE 34. SATELLITE IMAGE OF CYCLONE DEVELOPMENT, JULY 21, 1977, 1745 GMT.

Case of August 31

On September 1, a strong band of westerlies was manifest on the 500-mb chart along 45N (Figure 35) with an upper-low center near 52N 178E.

Visible satellite imagery of August 31 at 2315 GMT, showed a leaf-shaped cloud with a sharply defined back edge marked A (Figure 38) and a slot just beginning to form at B. A comma cloud marked C was circulating around the 500-mb low center. On the surface chart at 1200 GMT, a new wave was forming near 170W (Figure 36).

On enhanced IR imagery on September 1 at 0615 GMT, the leaf cloud, with its back edge marked A, had moved eastward about seven degrees (Figure 39). The comma cloud, marked C, was left behind. The leaf-cloud pattern suggested that the surface low would continue to deepen. By September 1 at 1200 GMT, the surface low center at 47N 155W had deepened to 1004 mb (Figure 37).

Enhanced satellite imagery on September 1 at 1515 GMT shows rapid development and eastward movement of the system (Figure 40). The head of the slot at B was seen to be moving 80 knots on movie loops! The speed of the surface low center was 50 knots. In this case, cyclogenesis could have been detected as early as 2315 GMT by examining the satellite pictures.

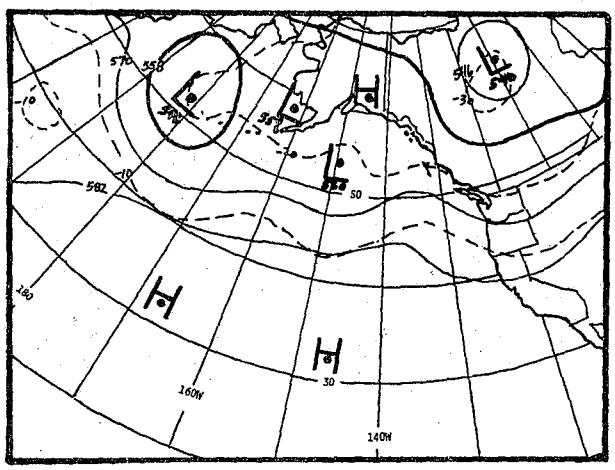

Figure 35. 500-mb Analysis, 9/1/77, 0000 GMT.

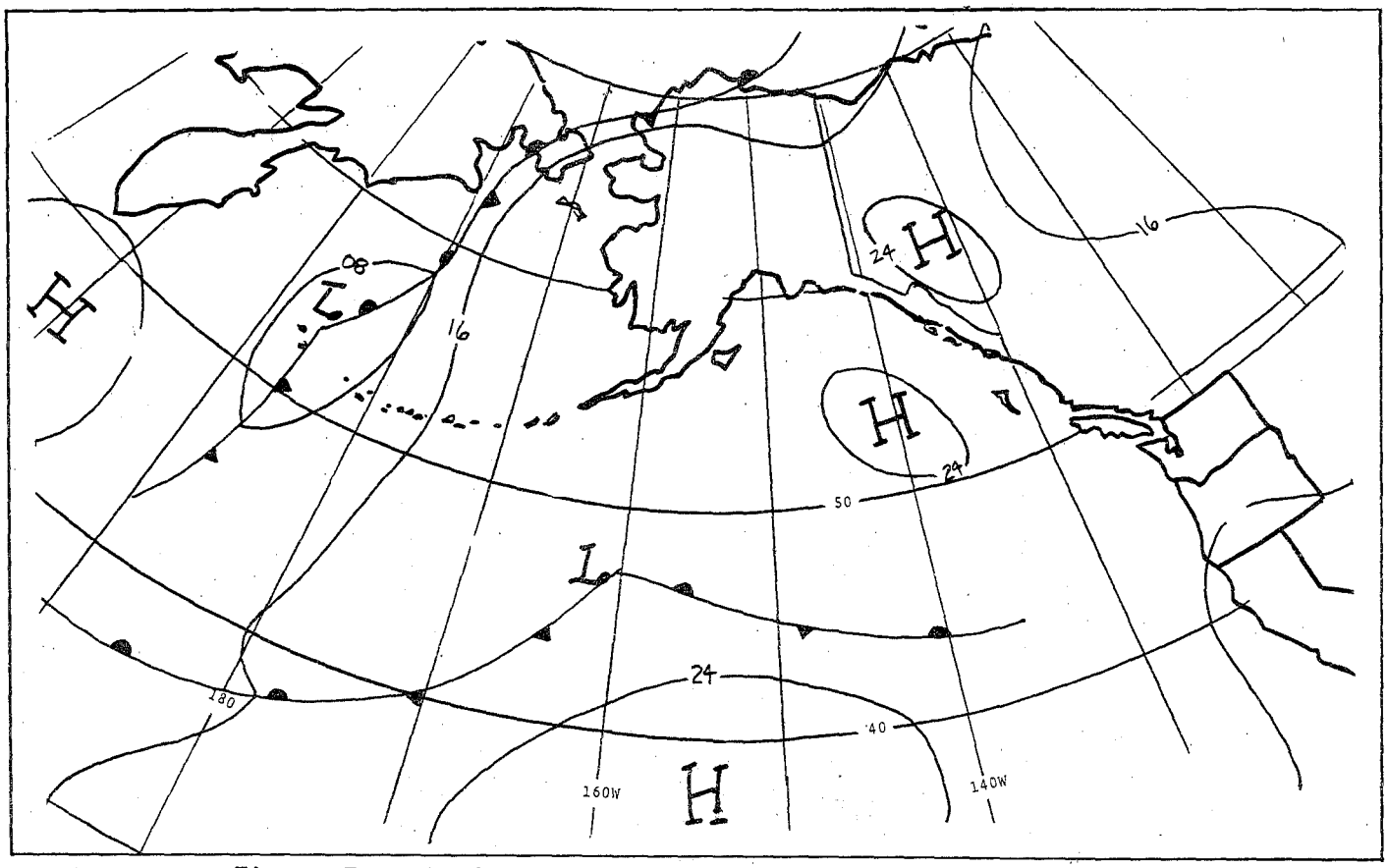

Figure 36. Surface Analysis, August 31, 1977, 1200 GMT.

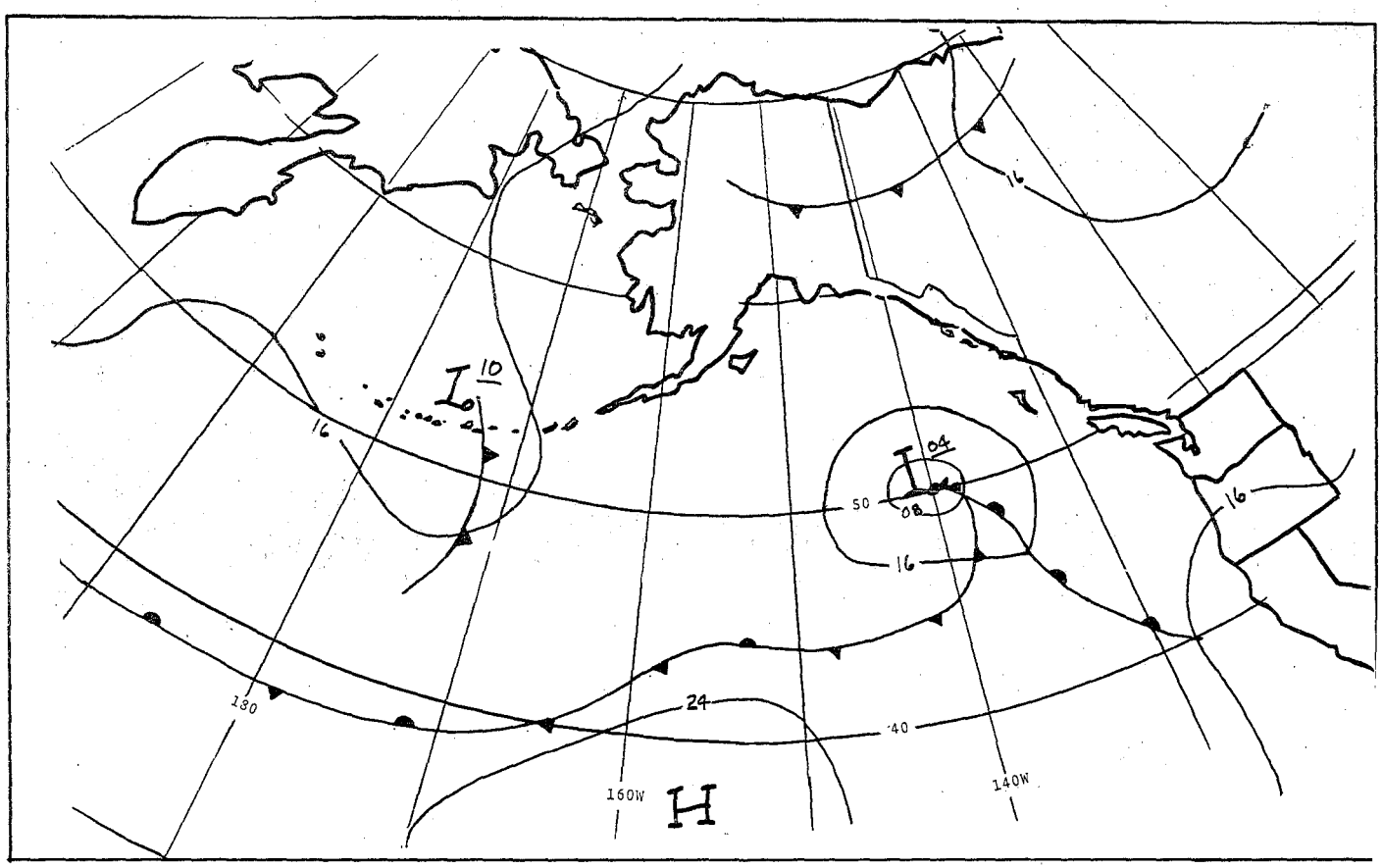

Figure 37. Surface Analysis, September 1, 1977, 1200 GMT.

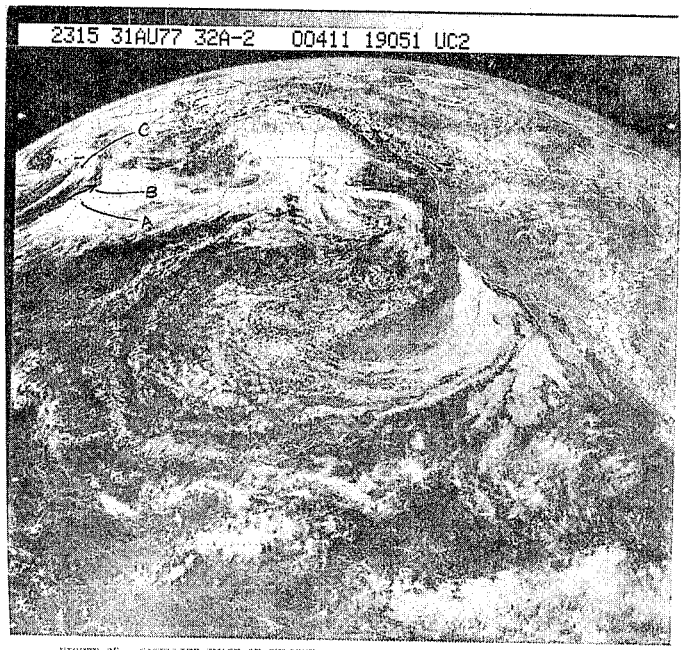

FIGURE 38. SATELLITE IMAGE OF CYLCONE DEVELOPMENT, AUGUST 31, 1977, 2315 GMT.

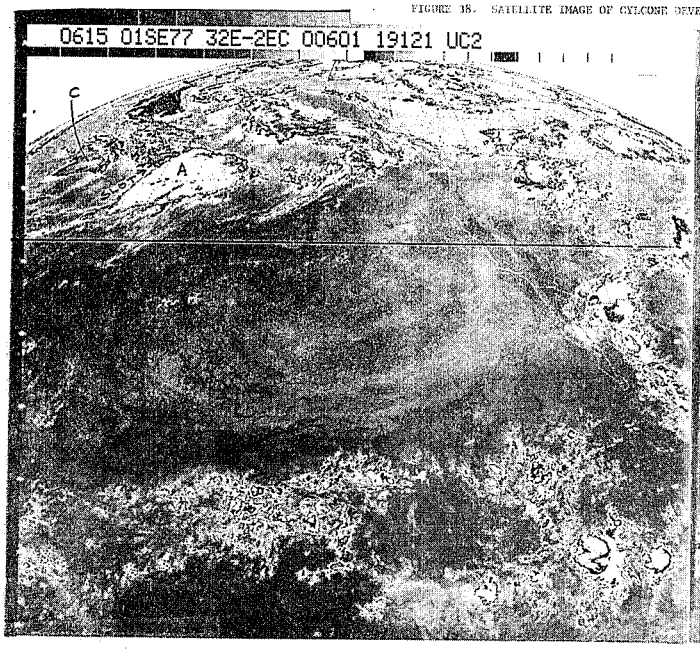

FIGURE 39. SATELLITE IMAGE OF CYCLONE DEVELOPMENT, SEPTEMBER 1, 1977, 0615 GMT.

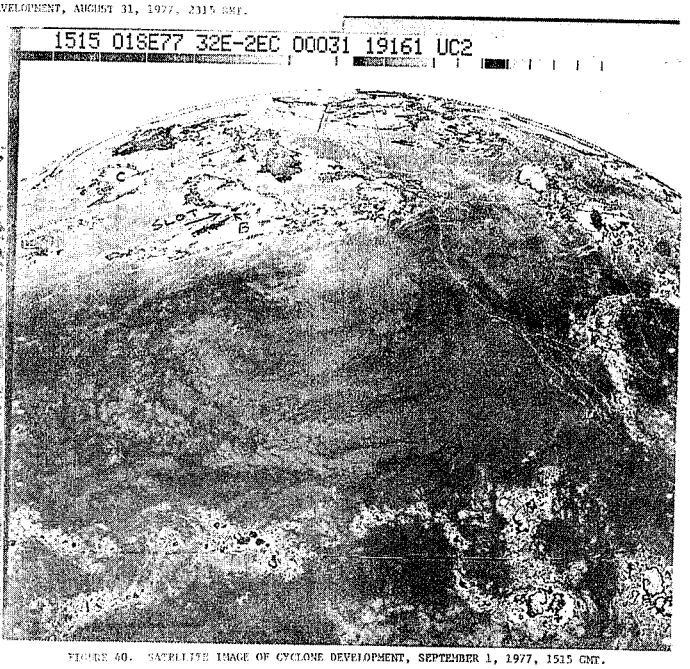

FIGURE 40. SATELLITE IMAGE OF CYCLONE DEVELOPMENT, SEPTEMBER 1, 1977, 1515 GMT.

Case of October 5

Development again occurred near the edge of the satellite picture where the image was distorted and difficult to read. There were two interconnected cloud patterns, labeled A and B, in Figure 44. System A was a closed, upper-level, low-pressure center that was quite weak (Figure 41). The surface cyclone labeled B was located at 55N 165W near the central Aleutians. The slot of this developing low center traveled northeastward. By 2345 GMT the slot had moved eastward to 55N 150W (Figure 46). A surface low center of 1004 mb located at 52N 170W on October 5 at 1200 GMT (Figure 42) continued to deepen to 994 mb as the slot grew larger (Figure 43). This slot was not discernible on the visible picture of 2315 GMT (Figure 45), but the jet-stream shadow (jet core) could be seen near A. Another cold front was located near point B on this same figure. Colder, more unstable air later moved into the surface low associated with system B, and it continued to deepen.

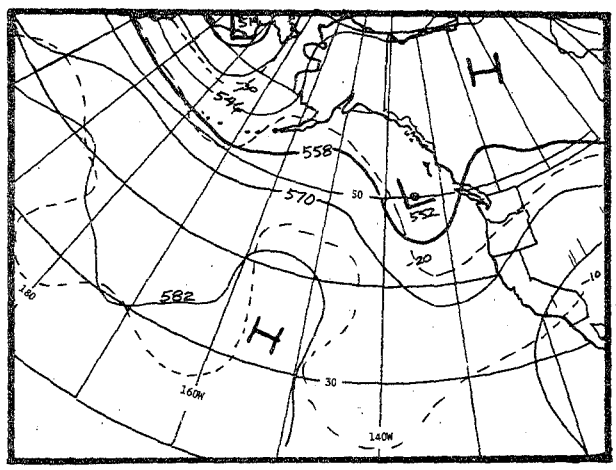

Figure 41. 500-mb Analysis, 10/6/77, 0000 GMT.

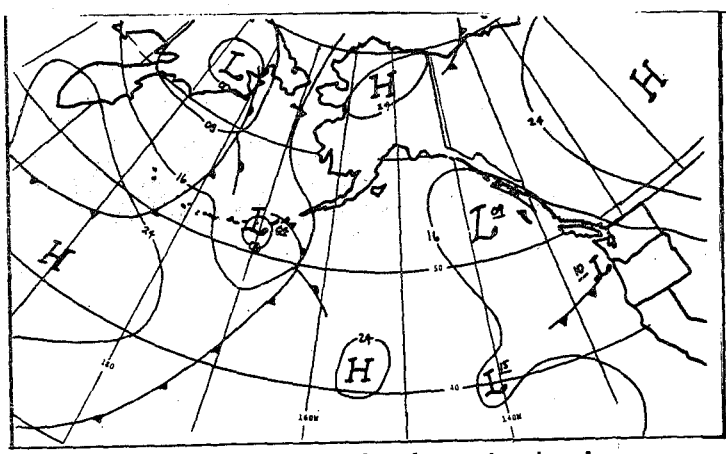

Figure 42. Surface Analysis, 10/5/77, 1200 GMT.

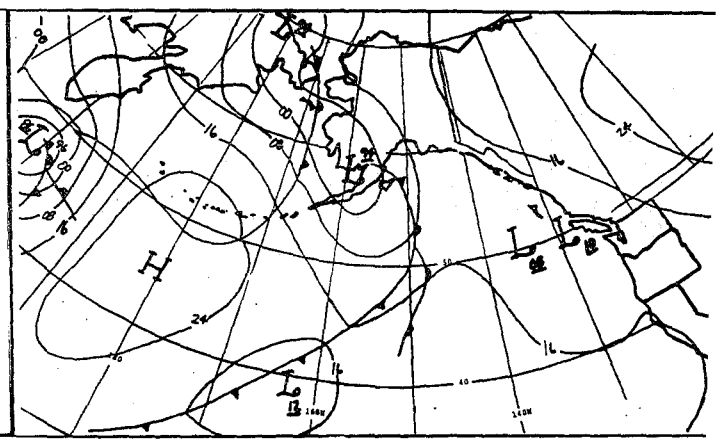

Figure 43. Surface Analysis, 10/6/77, 1200 GMT.

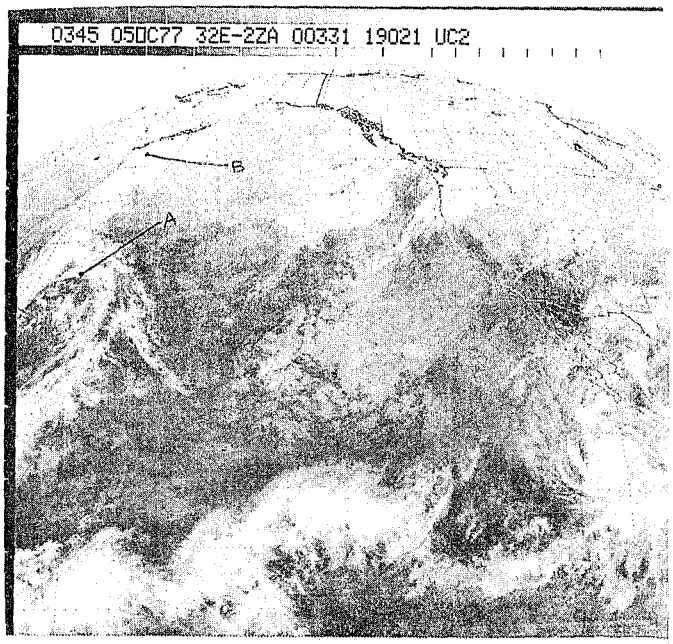

FIGURE 44. SATELLITE IMAGE OF CYCLONE DEVELOPMENT, OCTOBER 5, 1977, 0345 GMT.

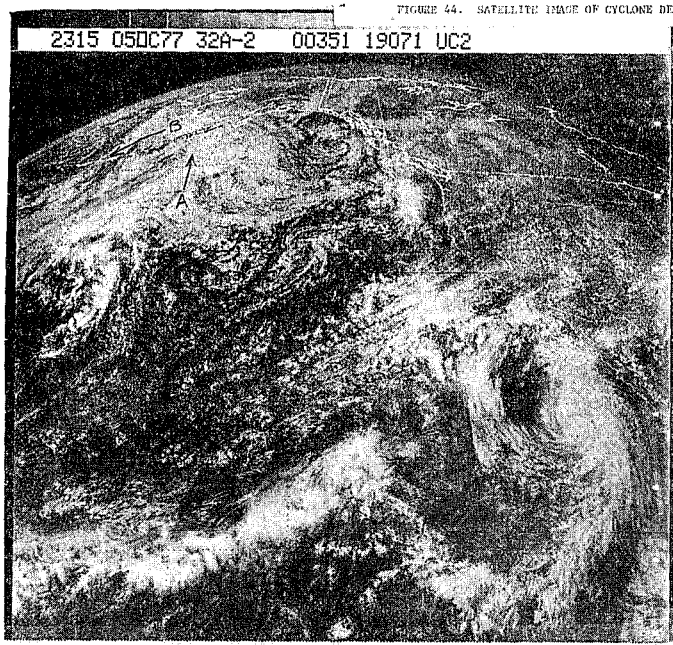

FIGURE 45. SATELLITE IMAGE OF CYCLONE DEVELOPMENT, OCTOBER 5, 1977, 2315 GMT.

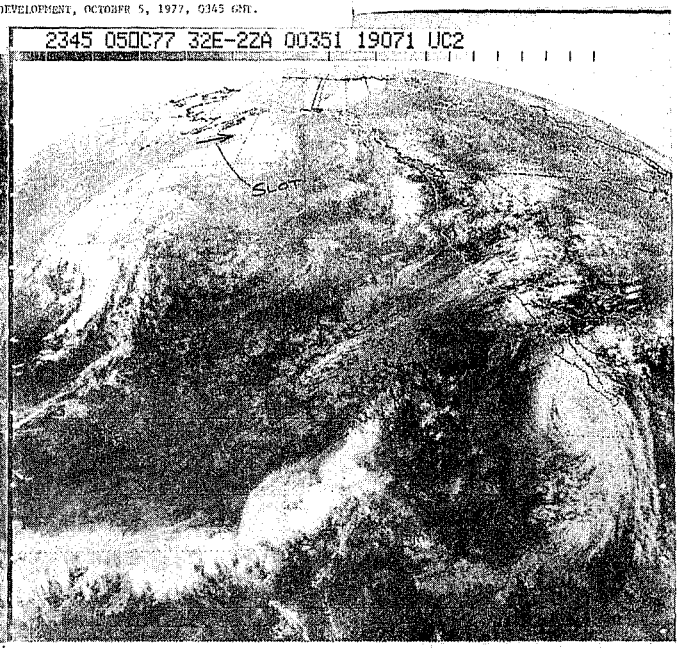

FIGURE 46. SATELLITE IMAGE OF CYCLONE DEVELOPMENT, OCTOBER 5, 1977, 2345 GMT.

Case of November 17

On November 18 at 1145 GMT (Figure 50), a large cluster of clouds is shown centered at 41N 162W. This cloud was followed by a weakening baroclinic zone located at 40N 155W. At 2345 GMT a major cloud band had formed from the cloud cluster (Figure 51), and the head of the comma cloud had completed one rotation. This is often the case when a storm reaches maturity. This system formed and became fully developed in just 12 hours! Central pressure of the surface low fell 12 mb to 968 mb, Figures 48 and 49.

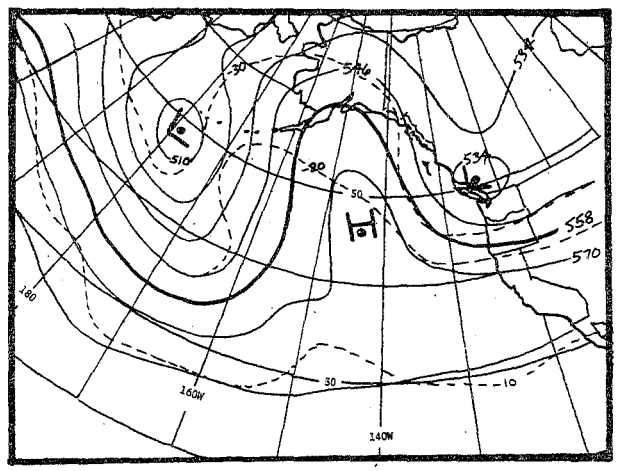

Figure 47. 500-mb Analysis, 11/18/77, 0000 GMT.

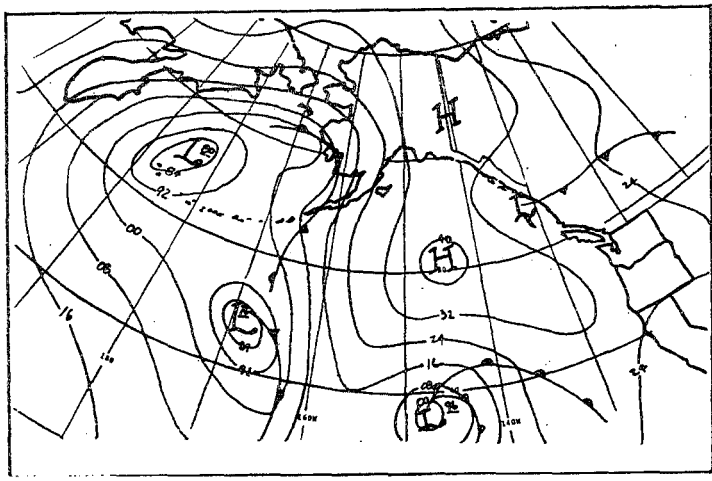

Figure 48. Surface Analysis, 11/17/77, 1200 GMT.

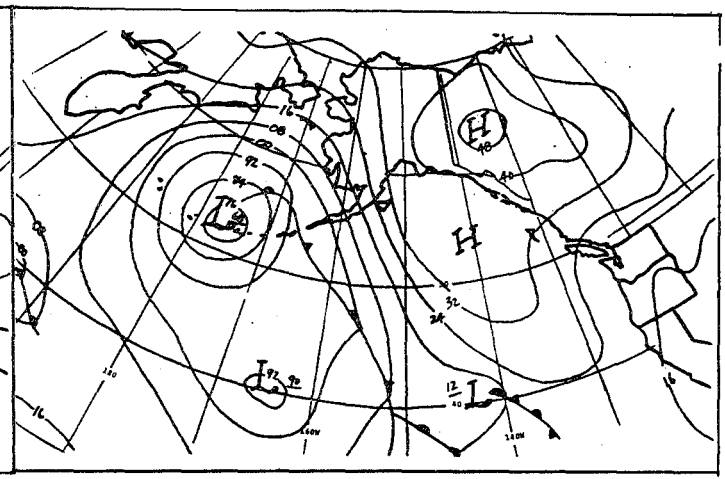

Figure 49. Surface Analysis, 11/18/77, 1200 GMT.

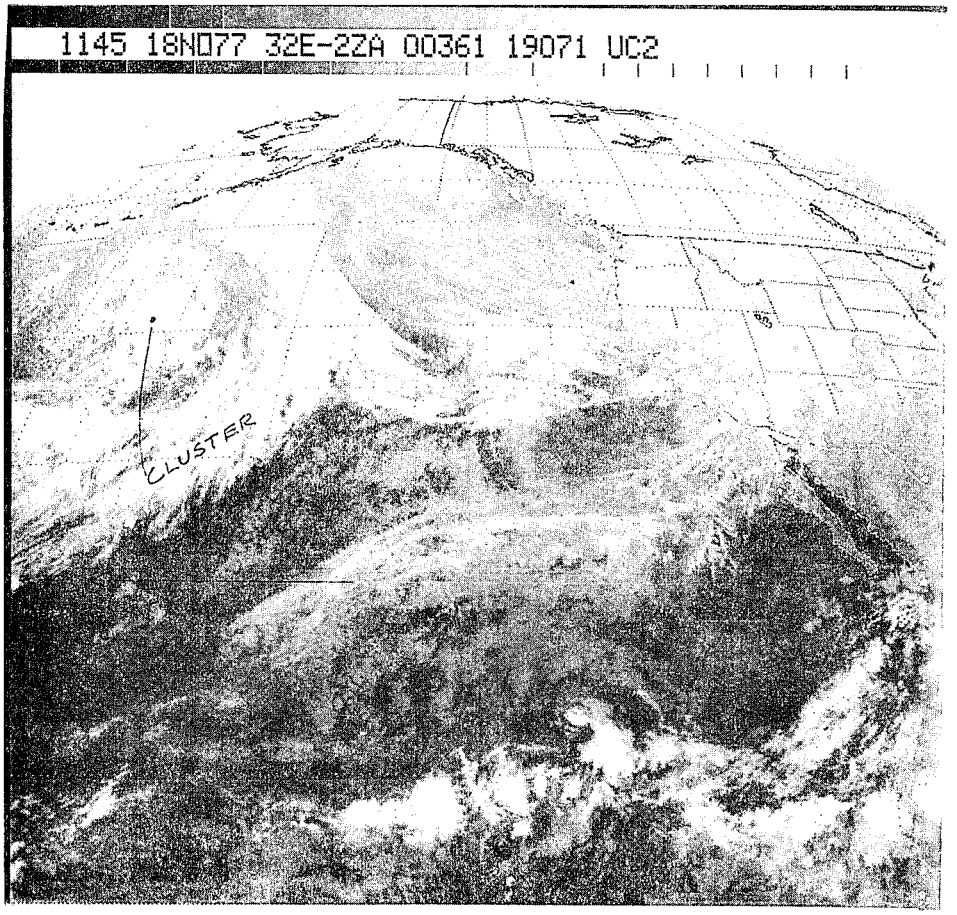

FIGURE 50. SATELLITE IMAGE OF CYCLONE DEVELOPMENT, NOVEMBER 18, 1977, 1145 GMT.

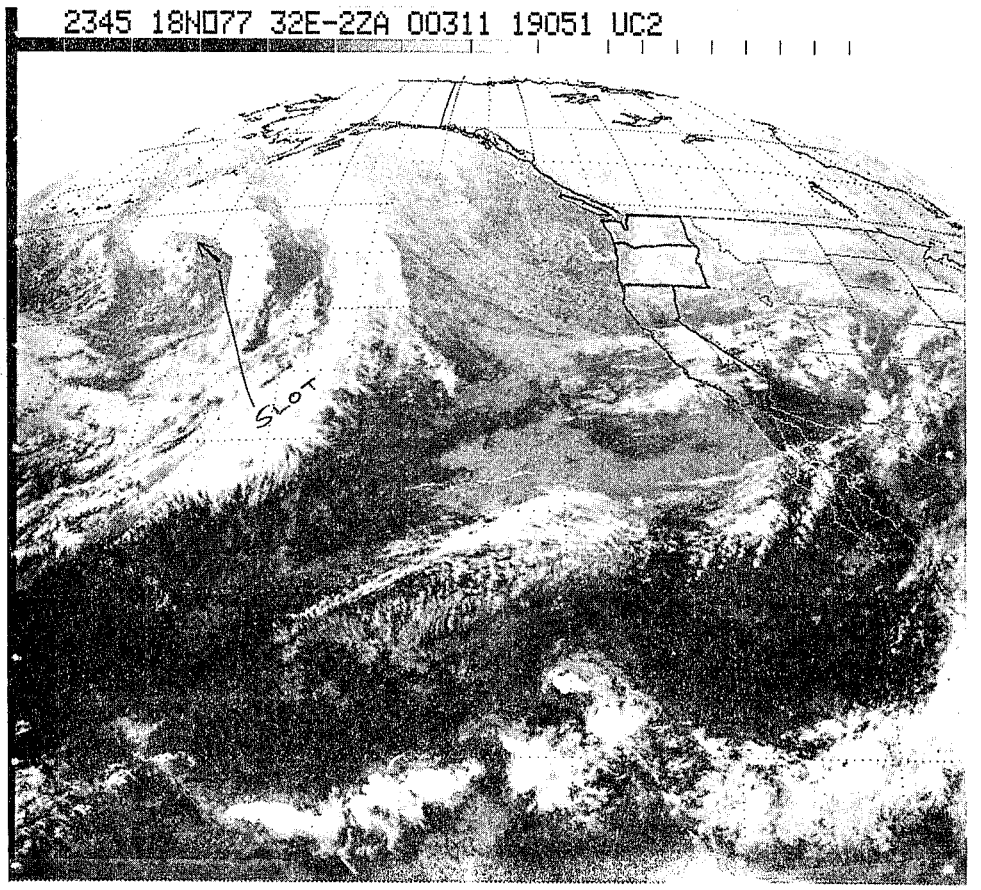

FIGURE 51. SATELLITE IMAGE OF CYCLONE [illegible], NOVEMBER

Cases of April 18, May 3, and September 25

Unfortunately, several of the 11 cases investigated were so near the edge of the satellite picture that they were difficult to study from the U. S. GOES-West satellite. Some of the features of the "ideal" case could be seen in these cases, but not all of them. The most common feature detectable in these as in nearly all the other cases was a distinct slot region, which appears to be the best evidence that cyclone deepening is taking place.

Satellite images for these cases are found in Figures 55, 56, 60, 61, 65, and 66. Surface and 500-mb charts for these cases are roughly similar to the other cases, and again the LFM prog failed to predict the cyclone deepening which took place (Figures 52-54, 57-59, 62-64).

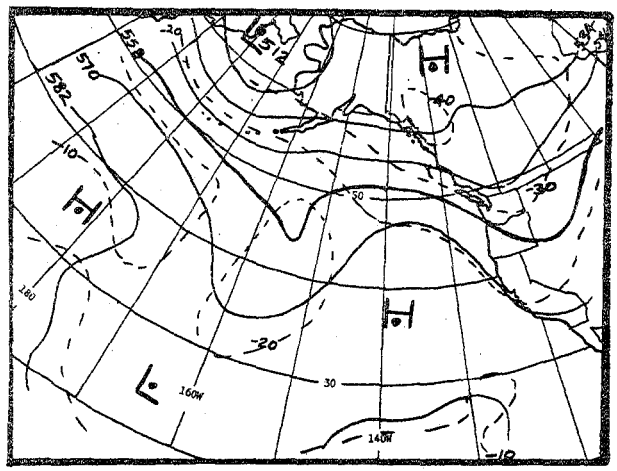

Figure 52. 500-mb Chart, 4/19/77, 0000 GMT.

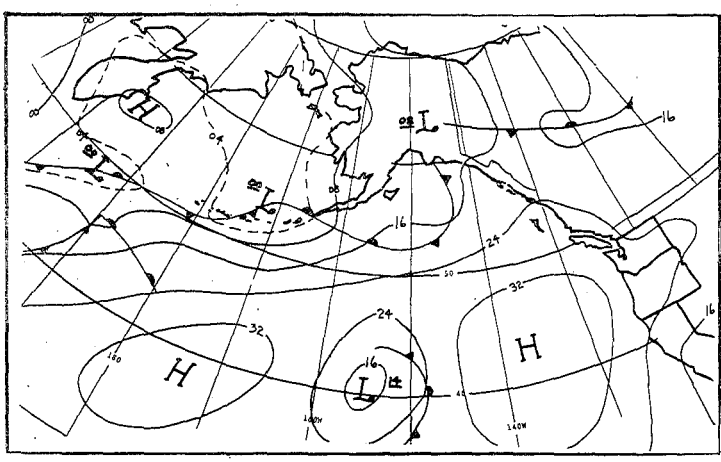

Figure 53. Surface Analysis, 4/18/77, 1200 GMT.

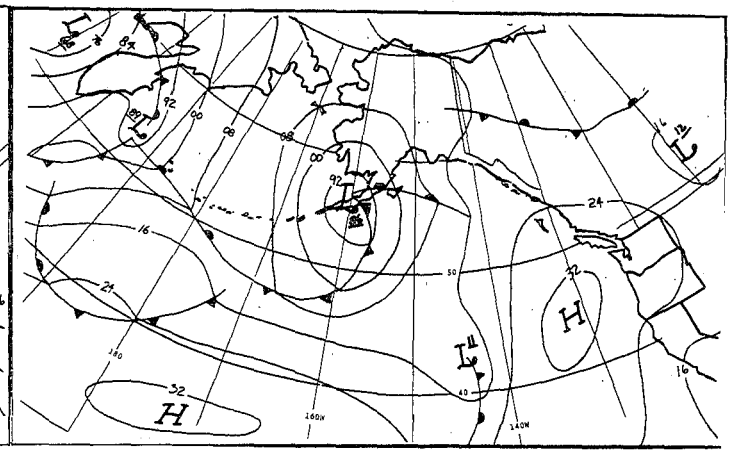

Figure 54. Surface Analysis, 4/19/77, 1200 GMT.

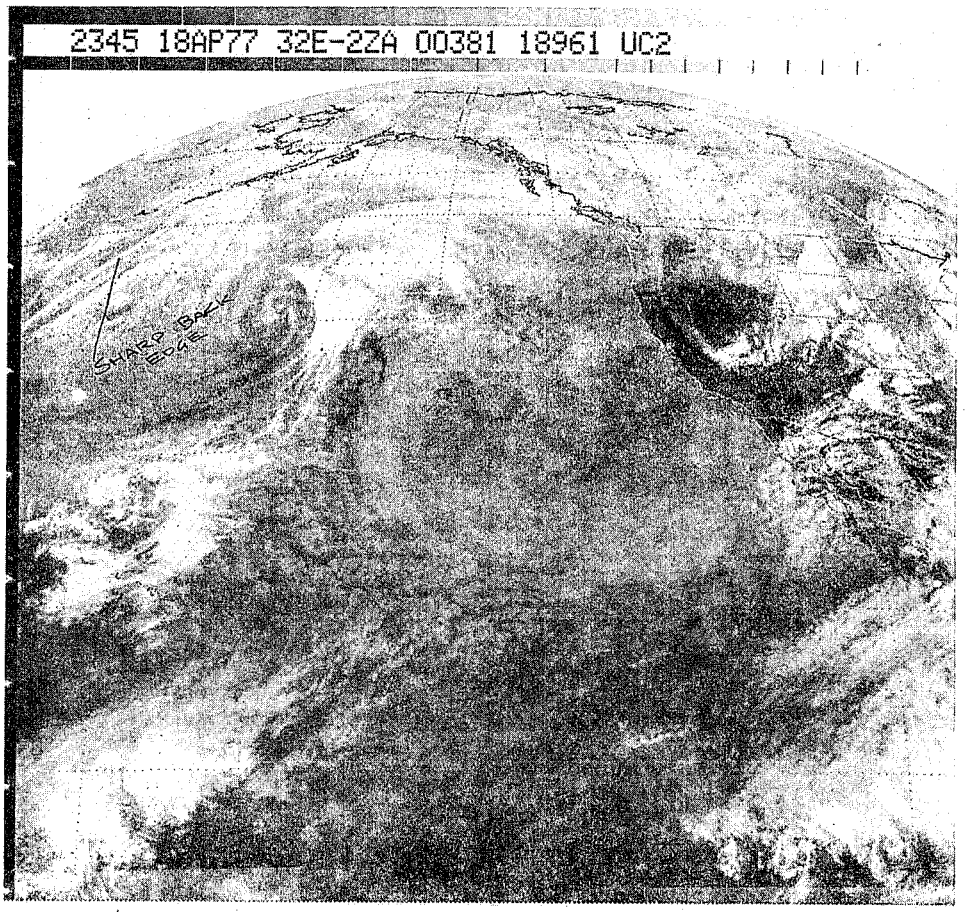

FIGURE 55. SATELLITE IMAGE OF CYCLONE DEVELOPMENT, APRIL 18, 1977, 2345 GMT.

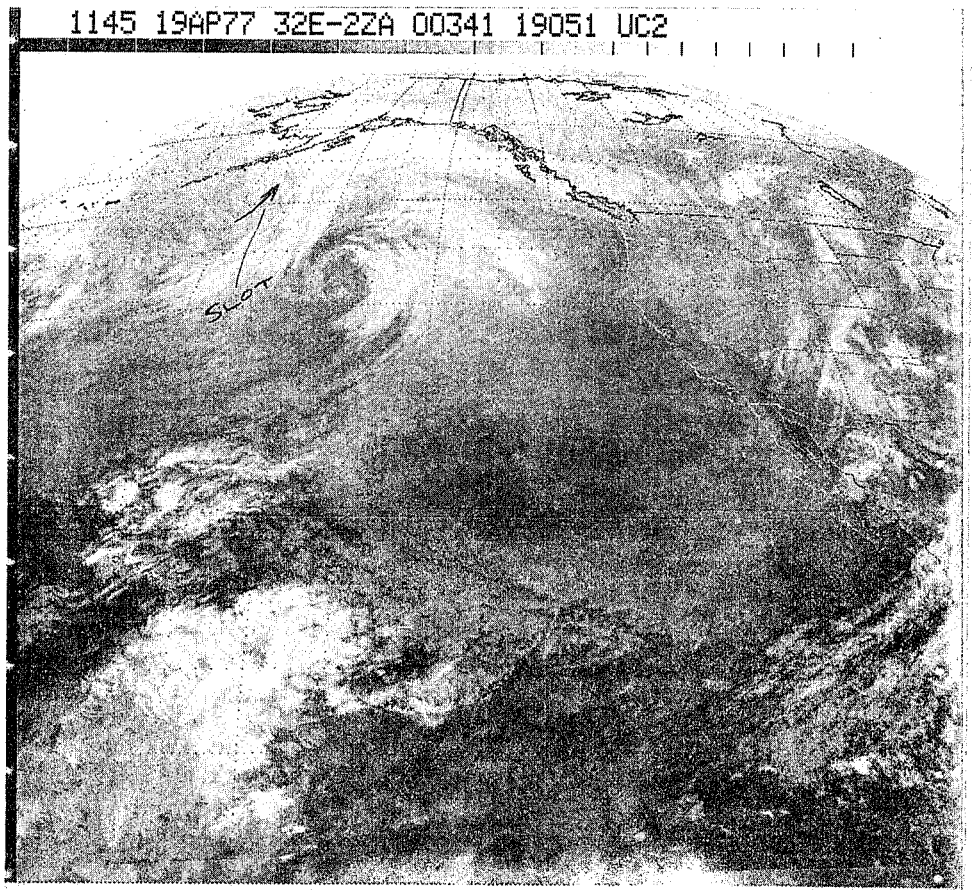

FIGURE 56. SATELLITE IMAGE OF CYCLONE DEVELOPMENT, APRIL [illegible] GMT.

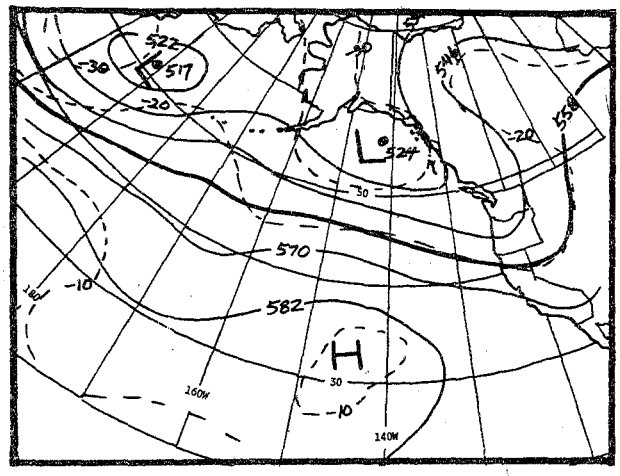

Figure 57. 500-mb Analysis, 5/4/77, 0000 GMT.

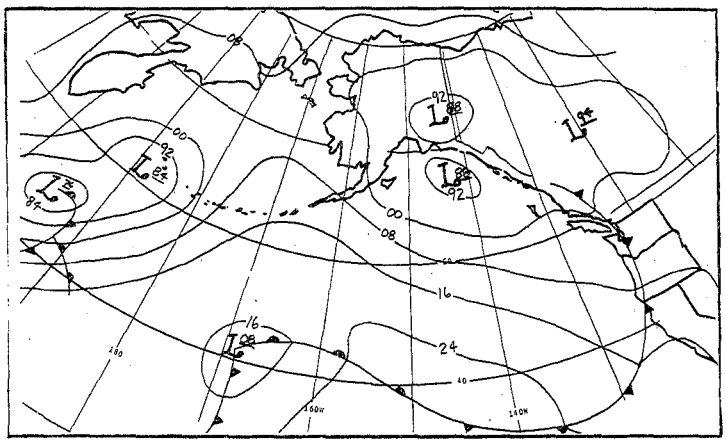

Figure 58. Surface Analysis, 5/3/77, 1200 GMT.

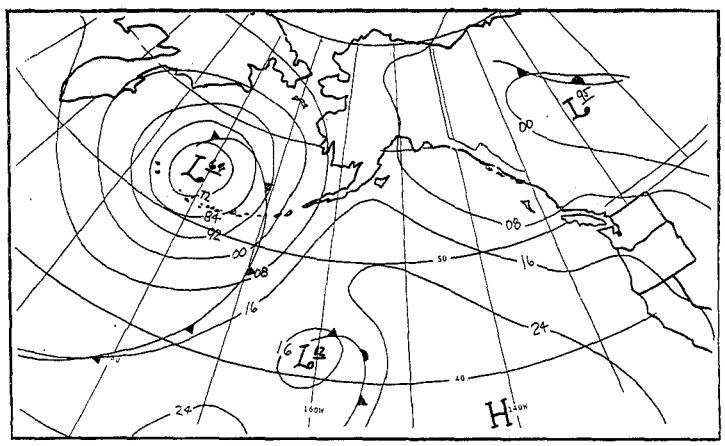

Figure 59. Surface Analysis, 5/4/77, 1200 GMT.

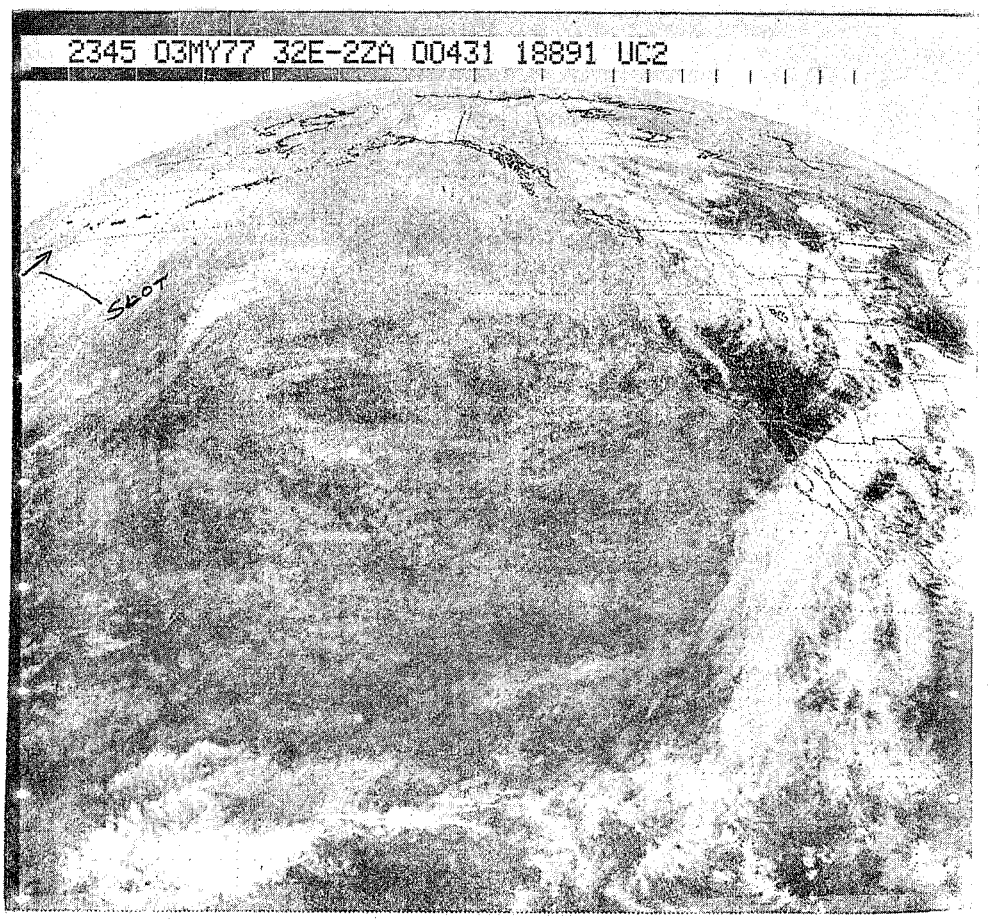

FIGURE 60. SATELLITE IMAGE OF CYCLONE DEVELOPMENT, MAY 3, 1977, 2345 GMT.

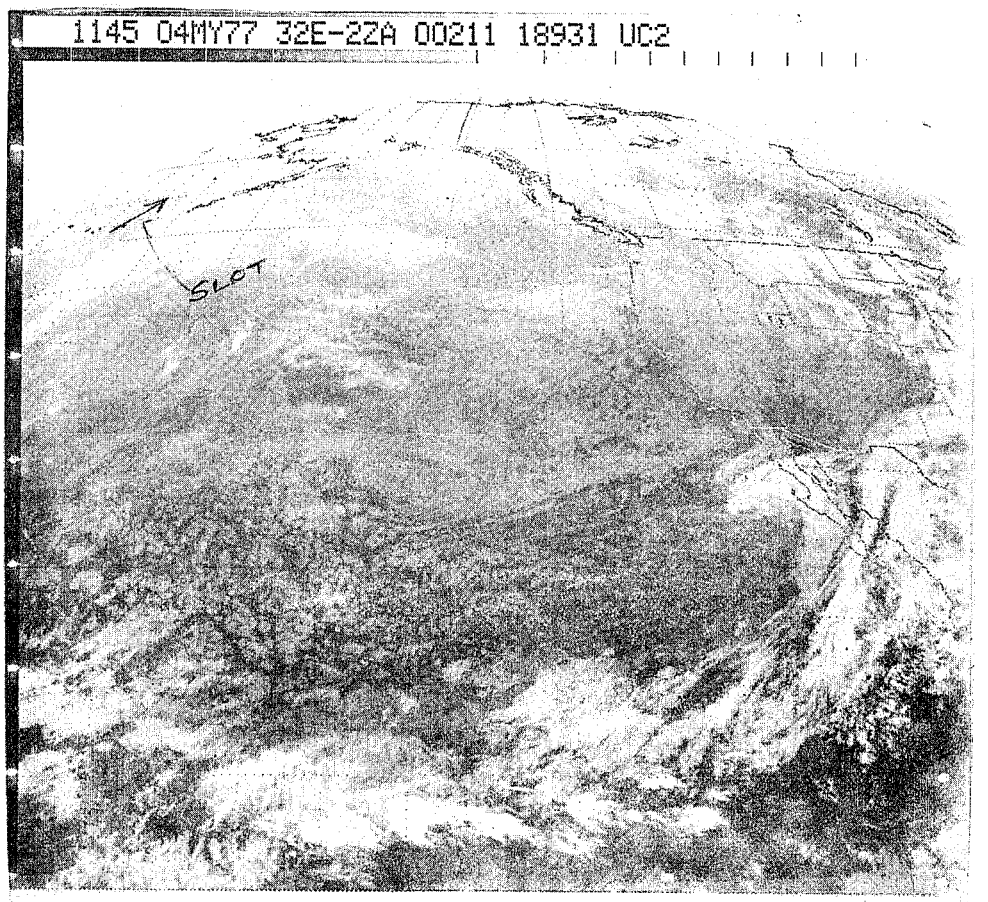

FIGURE 61. SATELLITE IMAGE OF CYCLONE DEVELOPMENT, [illegible]

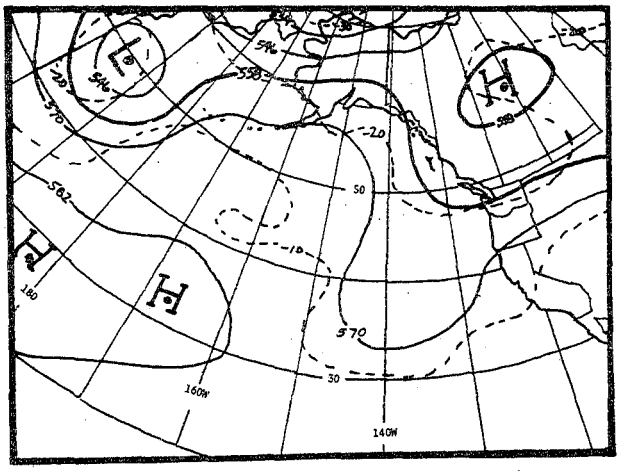

Figure 62. 500-mb Analysis, 9/26/77, 0000 GMT.

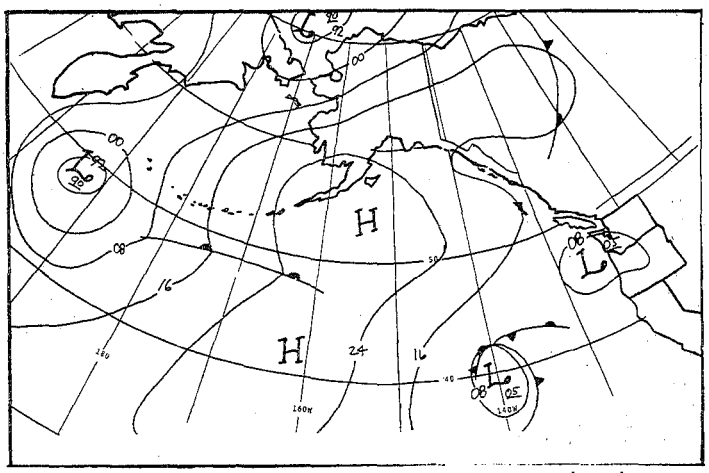

Figure 63. Surface Analysis, 9/25/77, 1200 GMT.

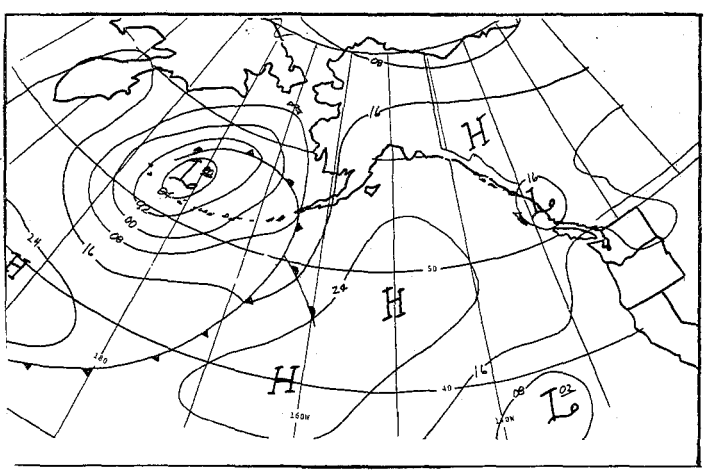

Figure 64. Surface Analysis, 9/26/77, 1800 GMT.

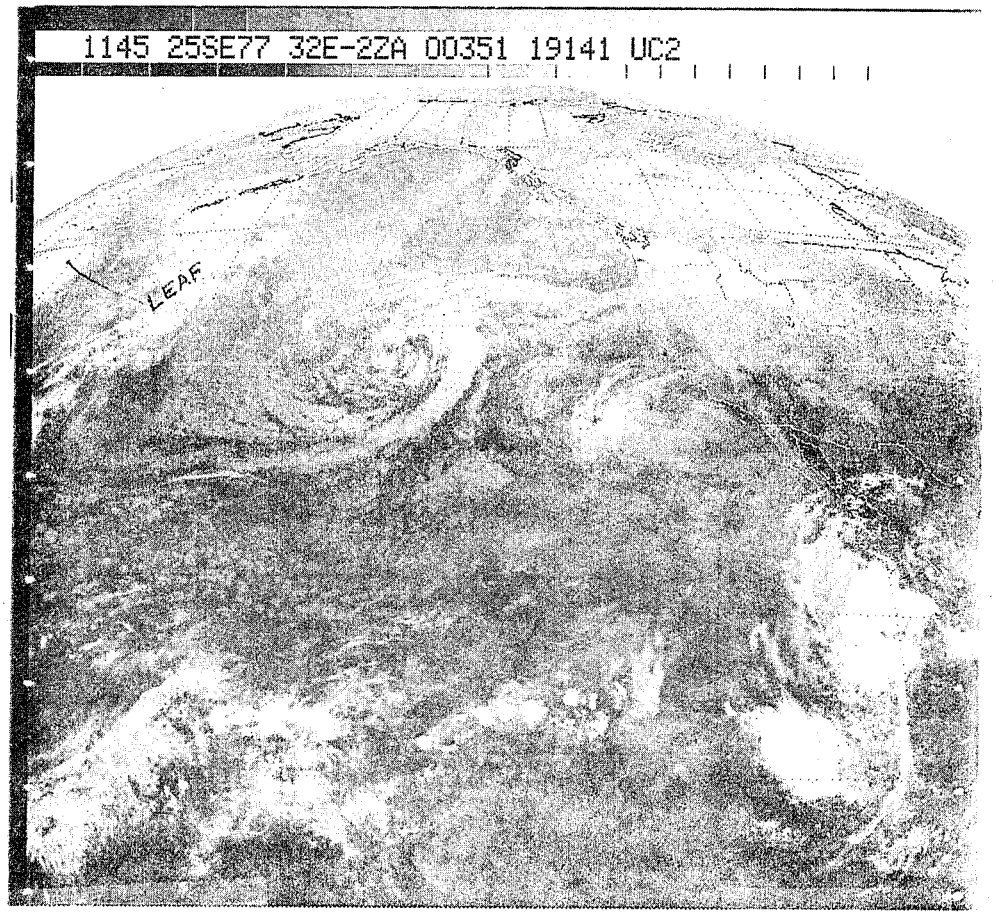

FIGURE 65. SATELLITE IMAGE OF CYCLONE DEVELOPMENT, SEPTEMBER 25, 1977, 1145 GMT.

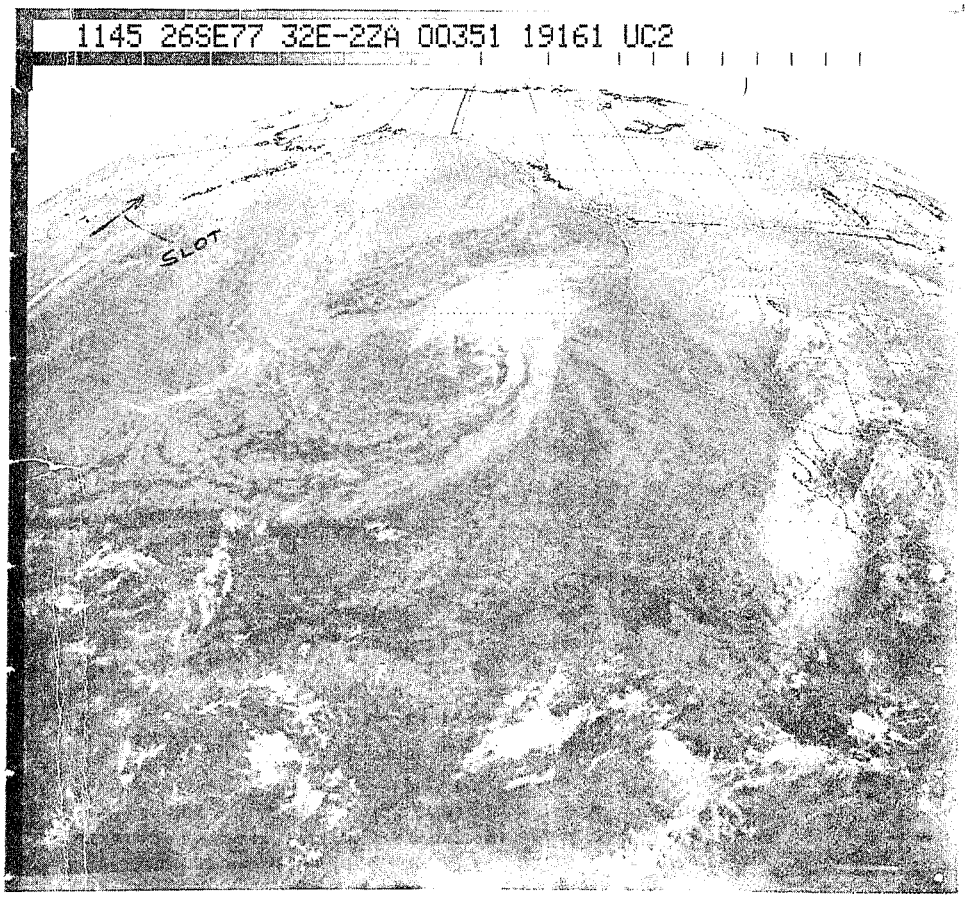

FIGURE 66. SATELLITE IMAGE OF CYCLONE DEVELOPMENT, SEPTEMBER 26, 1977, 1145 GMT.

VII. CONCLUSIONS

When making marine forecasts, location and intensity of cyclones must be accurately estimated. In the Eastern North Pacific, meteorologists should not hesitate to predict cyclone central pressure lower than indicated by LFM guidance whenever satellite evidence warrants it. The LFM, although a great help to the forecaster, is not perfect. Over a relatively short period (six months), there were a number of occurrences when LFM-predicted cyclone central pressure was in error by 10 mb or more. These errors made by the LFM may in part be due to an incorrect initial analysis.

The GOES IR satellite images which show initial development cyclone deepening night or day are of considerable assistance to the marine forecaster. The most consistent cloud feature associated with deepening cyclone systems is the slot. Slots form near the polar jet stream and usually extend from the upper troposphere to the surface. The sharpness of the back edge of the cloud boundary of the slot is a good clue that the surface cyclone is deepening. Shape and orientation of the slot indicate direction of movement of the system. Visible pictures also reveal slots; however, because of limited daylight in winter and low clouds which are sometimes present in the slot region, visible imagery is often not as reliable as IR images. IR-enhanced images are very helpful for determining slot location and characteristics of the slot provide important information. A ruffled slot boundary indicates a weakening and slow-moving cyclone. A spiral-shaped slot shows that a matured system has become nearly stationary. A speed maxima, indicated by cluster of rapidly moving high clouds, can cause the cyclone and associated frontal system to intensify when it moves near the slot region.

An area of open cellular clouds behind the slot indicates that the system will continue to deepen. Ridge development aloft is indicated by cirrus clouds overrunning open cellular clouds behind the slot. When this occurs, the system is no longer deepening and the cyclone will begin to fill rapidly.

In winter and spring months, on the cold side of the polar jet stream, satellite photos often show comma-shaped cloud patterns detached from the baroclinic zone. These features are usually not predicted by the LFM or PE (Reed 1977); however, they are significant in the analysis of surface charts and to marine forecasting.

Whether a cyclone is ideal or complex, an inexperienced forecaster can usually detect development of cyclones and its movement by looking at two or more satellite images over a two-hour period. A series of pictures over a 24-hour period or time-lapse images (film loop) is very helpful.

Full maturity of cyclones in some cases may take as long as five days. In a number of cases, however, cyclones can change significantly or reach maturity in only 12 hours. For these short time spans, the forecaster should use satellite imagery to refine computer predictions.

VIII. ACKNOWLEDGMENTS

The helpful assistance of the following people is gratefully acknowledged:

Marion L. Dombrowski . . . . typed and retyped manuscript.
Marsh McCord . . . . . figures and tables.
Arthur N. Hull . . . . . review of manuscript.
Matthew H. Kulawiec . . . . review of manuscript.
Kent Short . . . . . review of manuscript.

Additional review was provided by Len Snellman and staff, Scientific Services Division, Western Region Headquarters.

IX. REFERENCES

Anderson, R. K., J. P. Ashman, F. Bittner, G. R. Farr, E. W. Ferguson, J. T. Oliver, and A. H. Smith, 1969: Applications of Meteorological Satellite Data in Analysis and Forecasting. ESSA Technical Report NESC 51.

Cohen, D. L., 1976: High Level PVA Impulse is Intensified by Low-Level Old Frontal Occlusions. Satellite Applications Note 76/11.

Lilly, K. E., Jr., LCDR, 1976: Marine Weather and the Commercial Mariner NWS, SOSU, Seattle, Washington.

Reed, R. J.: Non-Frontal Cyclone Development IAGA/JAMAP, Seattle, Washington, August 22 - September 3, 1977.

Ruscha, C. P., Jr., 1976: Satellite Data Gives Early Warning. Western Region Technical Attachment No. 76-19.

Weldon, R. B., 1976: Unpublished Satellite Training Notes, National Environmental Satellite Service, NOAA.

Weldon, R. B., 1977: An Oceanic Cyclogenesis - Its Cloud Pattern Interpretation. Satellite Applications Note 77/7, National Environmental Satellite Service, NOAA.

Wisner, W. M., 1977: An Example of the Importance of Subsynoptic Features in Forecasting. Satellite Applications Note 77/11, National Environmental Satellite Service, NOAA.

Wright, Stanley, 1978: Cloud Systems Moving Within a Southern Branch of the Westerlies. Satellite Applications Note 78/2, National Environmental Satellite Service, NOAA.

NOAA Technical Memoranda NWSWR: (Continued)

92 Smoke Management in the Willamette Valley. Earl M. Bates, May 1974. (COM-74-11277/AS)
93 An Operational Evaluation of 500-mb Type Stratified Regression Equations. Alexander E. MacDonald, June 1974. (COM-74-11407/AS)
94 Conditional Probability of Visibility Less than One-Half Mile in Radiation Fog at Fresno, California. John D. Thorpe, August 1974. (COM-74-11955/AS)
95 Climate of Flagstaff, Arizona. Paul W. Sorenson, August 1974. (COM-74-11678/AS)
96 Map Type Precipitation Probabilities for the Western Region. Glenn E. Rasch and Alexander E. MacDonald, February 1975. (COM-75-10428/AS)
97 Eastern Pacific Cut-off Low of April 21-28, 1974. William J. Alder and George R. Miller, January 1976. (PB-250-711/AS)
98 Study on a Significant Precipitation Episode in the Western United States. Ira S. Brenner, April 1975. (COM-75-10719/AS)
99 A Study of Flash Flood Susceptibility--A Basin in Southern Arizona. Gerald Williams, August 1975. (COM-75-11560/AS)
100 A Study of Flash-Flood Occurrences at a Site Versus Over a Forecast Zone. Gerald Williams, Aug. 1975. (COM-75-11404/AS)
102 A Set of Rules for Forecasting Temperatures in Napa and Sonoma Counties. Wesley L. Tuft, Sr., 1975. (PB-246-902/AS)
103 Application of the National Weather Service Flash-Flood Program in the Western Region. Gerald Williams, January 1976. (PB-253-055/AS)
104 Objective Aids for Forecasting Minimum Temperatures at Reno, Nevada, During the Summer Months. Christopher D. Hill, January 1976. (PB-252-866/AS)
105 Forecasting the Mono Wind. Charles P. Ruscha, Jr., February 1976. (PB-254-630)
106 Use of MOS Forecast Parameters in Temperature Forecasting. John C. Plankinton, Jr., March 1976. (PB-254-649)
107 Map Types as Aid in Using 6-h PoPs in Western United States. Ira S. Brenner, August 1976. (PB-259-594)
108 Other Kinds of Wind Shear. Christopher D. Hill, August 1976. (PB-260-437/AS) (PB-273-677/AS),
109 Forecasting North Winds in the Upper Sacramento Valley and Adjoining Forests. Christopher E. Fontana, Sept. 1976.
110 Cool Inflow as a Weakening Influence on Eastern Pacific Tropical Cyclones. William J. Denney, November 1976. (PB-264-655/AS)
112 The MAN/MOS Program. Alexander E. MacDonald, February 1977. (PB-265-941/AS)
113 Winter Season Minimum Temperature Formula for Bakersfield, California, Using Multiple Regression. Michael J. Oard, February 1977. (PB-275-694/AS)
114 Tropical Cyclone Kathleen. James R. Fors, February 1977. (PB-273-676/AS)
116 A Study of Wind Gusts on Lake Mead. Bradley Colman, April 1977. (PB-268-847)
117 The Relative Frequency of Cumulonimbus Clouds at the Nevada Test Site as a Function of K-value. R. F. Quiring, April 1977. (PB-272-851)
118 Moisture Distribution Modification by Upward Vertical Motion. Ira S. Brenner, April 1977. (PB-268-740)
119 Relative Frequency of Occurrence of Warm Season Echo Activity as a Function of Stability Indices Computed from the Yucca Flat, Nevada, Rawinsonde. Darryl Randerson, June 1977. (PB-271-290/AS)
121 Climatological Prediction of Cumulonimbus Clouds in the Vicinity of the Yucca Flat Weather Station. R. F. Quiring, June 1977. (PB-271-704/AS)
122 A Method for Transforming Temperature Distribution to Normality. Morris S. Webb, Jr., June 1977. (PB-271-742/AS)
123 Study of a Heavy Precipitation Occurrence in Redding, California. Christopher E. Fontana, June 1977. (PB-273-624/AS)
124 Statistical Guidance for Prediction of Eastern North Pacific Tropical Cyclone Motion - Part I. Charles J. Neumann and Preston W. Leftwich, August 1977. (PB-272-661)
125 Statistical Guidance on the Prediction of Eastern North Pacific Tropical Cyclone Motion - Part II. Preston W. Leftwich and Charles J. Neumann, August 1977. (PB-273-152/AS)
126 Climate of San Francisco. E. Jan Null, March 1978. (PB-279-975/AS)
127 Development of a Probability Equation for Winter-Type Precipitation Patterns in Great Falls, Montana. Kenneth E. Mielke, February 1978. (PB-281-387/AS)
128 Hand Calculator Program to Compute Parcel Thermal Dynamics. Dan Gudgel, April 1978. (PB-283-080/AS)
129 Fire Whirls. David W. Goens, May 1978. (PB-285-868/AS)
130 Flash-Flood Procedure. Ralph C. Hatch and Gerald Williams, May 1978. (PB-286-014/AS)
131 Automated Fire-Weather Forecasts. Mark A. Mollner and David E. Olsen, September 1978. (PB-288-916/AS)
132 Estimates of the Effects of Terrain Blocking on the Los Angeles WSR-74C Weather Radar. R. G. Pappas, R. Y. Lee, and B. W. Finke, October 1978. (PB-289-767/AS)
133 Spectral Techniques in Ocean Wave Forecasting. John A. Jannuzzi, October 1978.
134 Solar Radiation. John A. Jannuzzi, November 1978.
135 Application of a Spectrum Analyzer in Forecasting Ocean Swell in Southern California Coastal Waters. Lawrence P. Kierulff, January 1979.
136 Basic Hydrologic Principles. Thomas L. Dietrich, January 1979.

NOAA SCIENTIFIC AND TECHNICAL PUBLICATIONS

NOAA, the *National Oceanic and Atmospheric Administration*, was established as part of the Department of Commerce on October 3, 1970. The mission responsibilities of NOAA are to monitor and predict the state of the solid Earth, the oceans and their living resources, the atmosphere, and the space environment of the Earth, and to assess the socioeconomic impact of natural and technological changes in the environment.

The six Major Line Components of NOAA regularly produce various types of scientific and technical information in the following kinds of publications:

PROFESSIONAL PAPERS — Important definitive research results, major techniques, and special investigations.

TECHNICAL REPORTS—Journal quality with extensive details, mathematical developments, or data listings.

TECHNICAL MEMORANDUMS — Reports of preliminary, partial, or negative research or technology results, interim instructions, and the like.

CONTRACT AND GRANT REPORTS—Reports prepared by contractors or grantees under NOAA sponsorship.

TECHNICAL SERVICE PUBLICATIONS—These are publications containing data, observations, instructions, etc. A partial listing: Data serials; Prediction and outlook periodicals; Technical manuals, training papers, planning reports, and information serials; and Miscellaneous technical publications.

ATLAS—Analysed data generally presented in the form of maps showing distribution of rainfall, chemical and physical conditions of oceans and atmosphere, distribution of fishes and marine mammals, ionospheric conditions, etc.

Information on availability of NOAA publications can be obtained from:

ENVIRONMENTAL SCIENCE INFORMATION CENTER
ENVIRONMENTAL DATA SERVICE
NATIONAL OCEANIC AND ATMOSPHERIC ADMINISTRATION
U.S. DEPARTMENT OF COMMERCE

3300 Whitehaven Street, N.W.
Washington, D.C. 20235